เซลล์แสงอาทิตย์ชนิดสีย้อมไวแสงที่มีไทเทเนียอิเล็กโตรดแบบพ่นเคลือบ

นาย ชัยวัฒน์ ศรีสมานุวัตร
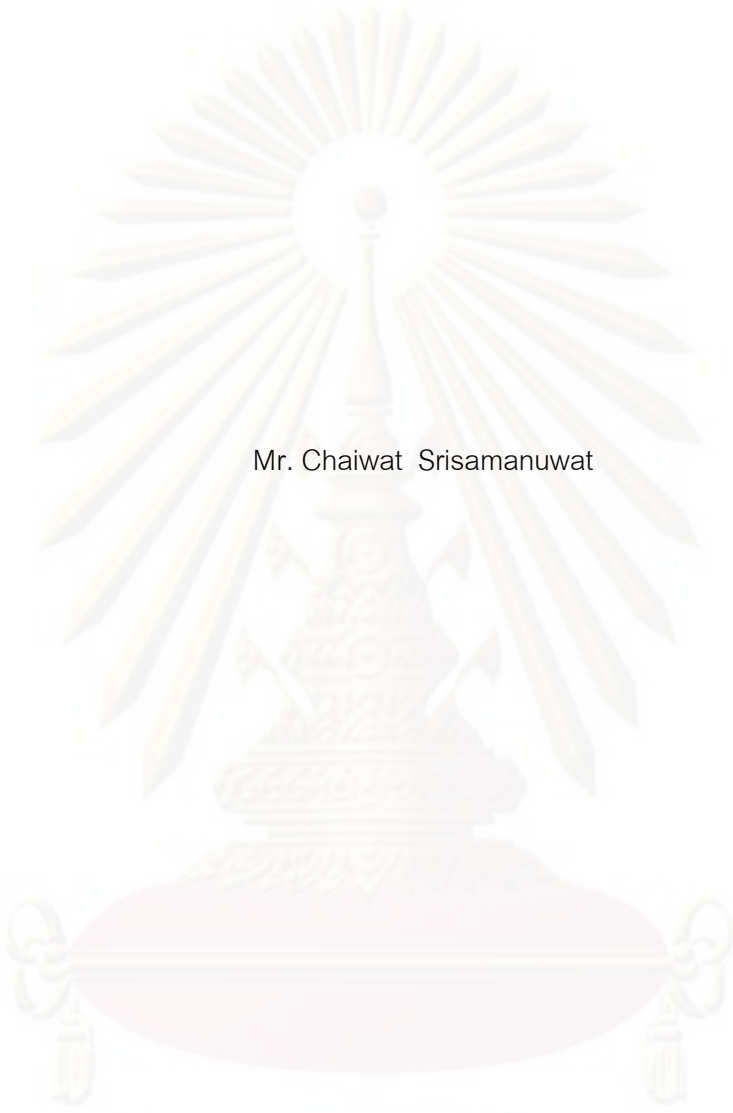
DYE-SENSITIZED SOLAR CELL WITH SPRAY COATED TiO$_2$ ELECTRODE

Mr. Chaiwat Srisamanuwat

A Thesis Submitted in Partial Fulfillment of the Requirements

for the Degree of Master of Engineering Program in Chemical Engineering

Department of Chemical Engineering

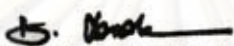Faculty of Engineering

Chulalongkorn University

Academic Year 2009

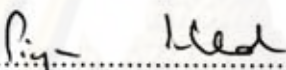Thesis Title   DYE-SENSITIZED SOLAR CELL WITH SPRAY COATED TiO$_2$
                                    ELECTRODE

By   Mr. Chaiwat Srisamanuwat

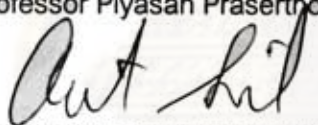Field of Study   Chemical Engineering

Thesis Advisor   Akawat Sirisuk, Ph.D.

Accepted by the Faculty of Engineering, Chulalongkorn University in Partial Fulfillment of the Requirements for the Master's Degree
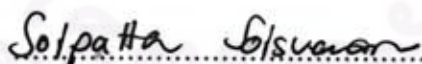
....Dean of the Faculty of Engineering

(Associate Professor Boonsom Lerdhirunwong, Dr.Ing.)

THESIS COMMITTEE

....Chairman

(Professor Piyasan Praserthdam, Dr.Ing.)

....Thesis Advisor

(Akawat Sirisuk, Ph.D.)

....Examiner

(Assistant Professor Joongjai Panpranot, Ph.D.)

....External Examiner

(Soipatta Soisuwan, D.Eng.)

ชัยวัฒน์ ศรีสมานุวัตร : เซลล์แสงอาทิตย์ชนิดสีย้อมไวแสงที่มีไทเทเนียอิเล็กโตรดแบบพ่น เคลือบ (DYE-SENSITIZED SOLAR CELL WITH SPRAY COATED TiO$_2$ ELECTRODE) อ. ที่ปรึกษาวิทยานิพนธ์หลัก: อ.ดร.อัครวัต ศิริสุข, 65 หน้า.

งานวิจัยนี้ได้ทำการศึกษาเซลล์แสงอาทิตย์ชนิดสีย้อมไวแสงที่มีไทเทเนียอิเล็กโตรดแบบ พ่นเคลือบโดยเตรียมไทเทเนียด้วยวิธีโซลเจลแล้วนำมาเคลือบลงบนกระจกด้วยเครื่องพ่นอัลตร้า โซนิค ส่วนประกอบอื่นๆของเซลล์แสงอาทิตย์ชนิดสีย้อมไวแสงคือ สีย้อมไวแสงชนิด N3 สารละลายอิเล็กโตรไลต์มีส่วนประกอบของคู่ปฏิกิริยารีดอกซ์ของไอโอไดด์/ไตรไอโอไดด์ การพ่น ฟิล์มแพลตินัมบนกระจกนำไฟฟ้าเป็นเคาน์เตอร์อิเล็กโตรด งานวิจัยนี้ศึกษาผลของอุณหภูมิในการ เผาและความหนาของชั้นฟิล์มของไทเทเนียฟิล์มที่มีผลต่อประสิทธิภาพของเซลล์แสงอาทิตย์ จาก การทดลองของไทเทเนียฟิล์มแบบชั้นเดียวพบว่า จะให้ประสิทธิภาพสูงสุดที่อุณหภูมิการเผา 400 องศาเซลเซียส วัดความหนาได้ประมาณ 11.1 ไมโครเมตร มาจากอุณหภูมิในการเผาที่สูงขึ้นจะ ช่วยทำให้ความหนาแน่นกระแสไฟฟ้าลัดวงจรเพิ่มขึ้น ซึ่งเป็นผลมาจากการเพิ่มขึ้นของความเป็น ผลึก แม้ว่าปริมาณการดูดซับโมเลกุลสีย้อมที่อุณหภูมิ 400 องศาเซลเซียสจะต่ำกว่าที่อุณหภูมิ 300 องศาเซลเซียส เมื่อนำไทเทเนียแบบสองชั้นมาเป็นอิเล็กโตรดประสิทธิภาพเซลล์จะสูงกว่า เมื่อเทียบกับไทเทเนียอิเล็กโตรดแบบชั้นเดียว ที่มีพื้นที่ผิวใกล้เคียงกัน ไทเทเนียอิเล็กโตรดแบบ สองชั้นจะช่วยทำให้การกระเจิงของแสงดีขึ้น ประสิทธิภาพเซลล์แสงอาทิตย์ที่มีไทเทเนียอิเล็กโตรด แบบสองชั้นมีค่าสูงสุดเมื่อชั้นแรกเผาด้วยอุณหภูมิ 400 องศาเซลเซียสเป็นเวลา 2 ชั่วโมงและชั้นที่ สองเผาด้วยอุณหภูมิ 350 องศาเซลเซียสเป็นเวลา 15 นาที ที่ความหนา 11.1 ไมโครเมตร

ภาควิชา..........วิศวกรรมเคมี..............ลายมือชื่อนิสิต....ชัยวัฒน์ ศรีสมานุวัตร.....

สาขาวิชา.......วิศวกรรมเคมี..............ลายมือชื่อ อ.ที่ปรึกษาวิทยานิพนธ์หลัก............

ปีการศึกษา...2552.............

##5170559521: MAJOR CHEMICAL ENGINEERING

KEYWORDS: DYE-SENSITIZED SOLAR CELL/ SPRAY-COATED / EFFICIENCY

CHAIWAT SRISAMANUWAT: DYE-SENSITIZED SOLAR CELL WITH SPRAY COATED TiO_2 ELECTRODE THESIS ADVISOR: AKAWAT SIRISUK, Ph.D.,65 pp.

Dye-sensitized solar cells (DSSC) with spray-coated TiO_2 electrode were studied. TiO_2 was prepared by a sol-gel method and was sprayed onto a conducting glass using an ultrasonic spray coater. Other components of the DSSC included N3 dye as a sensitizer, iodide/triiodide redox couple as an electrolyte, and a sputtered platinum film on conducting glass as a counter electrode. The effects of sintering temperature and thickness on the efficiency of the dye-sensitized solar cell were investigated. The highest efficiency of single-layered TiO_2 electrode was obtained when sintering temperature was $400^{\circ}C$ and the thickness of TiO_2 film was approximately 11.1 μm. Raising the sintering temperature increased the short-circuit current density due to increases in crystallinity and interparticle connections, in spite of the fact that the amount of dye adsorbed on the electrode sintered at $400^{\circ}C$ was less than that on the electrode sintered at $300^{\circ}C$. When a double-layered TiO_2 electrode was employed, the efficiency of the solar cell was higher, compared to a single-layered TiO_2 electrode with similar specific surface area. Double-layered TiO_2 electrode was fabricated to increase the light scattering. The highest efficiency of the solar cell with a double-layered TiO_2 electrode was obtained when the first layer of the electrode was sintered at $400^{\circ}C$ for two hours and the second layer was sintered at $350^{\circ}C$ for 15 minutes with a thickness of ca. 11.1 μm.

Department:...........Chemical Engineering.....Student's Signature................

Field of Study:........Chemical Engineering.....Advisor's Signature................

Academic Year:......2009.............

ACKNOWLEDGEMENTS

CONTENTS

LIST OF TABLES

Table   Page

LIST OF FIGURES

CHAPTER I

INTRODUCTION

Dye-sensitized solar cell (DSSC) is an electrochemical solar cell. The prototype of a dye-sensitized TiO_2 nanocrystalline solar cell was first reported by O'Regan and Gratzel in 1991(O'Regan and Gratzel., 1991). The DSSC have been recognized for their high efficiency on converting light into electricity by using readily available and environmentally friendly materials. DSSC attracted much attention due to their relatively high efficiency and low cost in comparison to conventional silicon-based solar cells.

DSSC consists of three main components: a dye-covered nanocrystalline TiO_2 layer on a transparent conductive glass substrate, an electrolyte contained iodide/ iodine redox couple, and a platinized conductive glass substrate as a counter electrode. Counter electrode, as one important component in DSSCs, is usually constructed with a conducting glass substrate coated with platinum film. The roles of the counter electrode are to collect electrons from external circuit and reduce I_2 to I^- in electrolyte to keep a low overvoltage and lessen energy losses (Macyk et al., 2007). Platinized counter electrode has low resistance and high electrocatalytic activity in DSSC. But platinum is one of the costly precious metals.

A transparent conducting substrate can be prepared by chemical vapor deposition, sputtering, spray pyrolysis, electron beam evaporation, and oxygen ion beam-assisted deposition. General requirements for transparent conducting glasses are low electrical resistivity and high transparency in visible spectral region. TiO_2 has been prepared by various methods such as a hydrothermal route using $TiCl_4$, flame hydrolysis of titanium tetraisopropoxide, sol-gel method through titanium tetrabutoxide.

Many research groups have focused on improving the photocurrent and photovoltage by developing new dye-sensitizers, improving the interfacial interaction and/or modifying the electrolyte components (Krebs et al., 2006). The energy conversion efficiency is likely to be dependent on the morphology and structure of the dye-adsorbed TiO_2 film. The nanoporous nature of the TiO_2 layer provides high surface area that is of great importance to the efficient photon-to-electricity conversion because it enhances dye loading and solar light absorption.

Several studies on the improvement of the light harvest efficiency of dye-adsorbed TiO_2 electrodes by light scattering. Using a TiO_2 layer with a higher surface area increases the dye adsorption, and such a higher surface area is usually obtained by using smaller particle sizes. The usual consequence is films which are relatively transparent, but which exhibit poor light scattering .Light scattering can be achieved by the presence of additional scattering layers in the TiO_2 layer (Lee et al., 2008).

The objective of this work is to study of the effect of sintering temperature and thickness of TiO_2 film on the efficiency of dye-sensitized solar cell for single-layer and double-layer TiO_2 films. The cell contained a spray-coated TiO_2 electrode prepared from titania sol. The photovoltaic performance of dye-sensitized solar cell was determined using the I-V tester.

The objectives of this research are as follows.

1. To study of the effect of sintering temperature and thickness of TiO_2 electrode layer on the efficiency of dye-sensitized solar cell.
2. To improve efficiency of dye-sensitized solar cell by employing double layer configuration for TiO_2 electrode.

This thesis is arranged as follows.

Chapter I is the introduction of this study.

Chapter II explains basic principles of dye-sensitized solar cell and information about TiO_2 and its preparation via a sol-gel method.

Chapter III reviews previous works related to this research.

Chapter IV describs the synthesis of the TiO_2 sol, the fabrication of dye-sensitized solar cell, and the characterization techniques used in this study.

Chapter V presents experimental results and discussion of this research.

In the last chapter, Chapter VI, overall conclusions of this research and recommendations for future work are given.

CHAPTER II

THEORY

2. Dye-sensitized solar cell (DSSC)

A dye-sensitized solar cell (DSSC) is a relatively new class of low-cost solar cell, which belongs to the group of thin film solar cells. The cell is based on a semiconductor formed between a photo-sensitized anode and an electrolyte as a photoelectrochemical system. This cell was invented by Michael Grätzel and Brian O'Regan in 1991 and is also known as Grätzel cells.

2.1 History of the Solar Cell

The photovoltaic effect was first reported by Edmund Bequerel in 1839 when he observed that the action of light on a silver coated platinum electrode immersed in electrolyte produced an electric current. Forty years later the first solid state photovoltaic devices were constructed by workers investigating the recently discovered photoconductivity of selenium. In 1876 William Adams and Richard Day found that a photocurrent could be produced in a sample of selenium when contacted by two heated platinum contacts. The photovoltaic action of the selenium differed from its photoconductive action in that a current was produced spontaneously by the action of light. No external power supply was needed. In this early photovoltaic device, a rectifying junction had been formed between the semiconductor and the metal contact. In 1894, Charles Fritts prepared what was probably the first large area solar cell by pressing a layer of selenium between gold and another metal. In the following years photovoltaic effects were observed in copper-copper oxide thin film structure, in lead sulphide and thallium sulphide. These early cells were thin film Schottky barrier devices, where a semitransparent layer of metal deposited on top of the semiconductor provided

both the asymmetric electronic junction, which is necessary for photovoltaic action, and access to the junction for the incident light. The photovoltaic effect of structures like this was related to the existence of a barrier to current flow at one of the semiconductor-metal interfaces (i..e., rectifying action) by Goldman and Brodsky in 1914. Later, during the 1930s, the theory of metal-semiconductor barrier layers was developed by Walter Schottky, Neville Mott and others.

However, it was not the photovoltaic properties of materials like selenium which excited researchers, but the photoconductivity. The fact that the current produced was proportional to the intensity of the incident light, and related to the wavelength in a definite way meant that photoconductive materials were ideal for photographic light meters. The photovoltaic effect in barrier structures was an added benefit, meaning that the light meter could operate without a power supply. It was not until the 1950s, with the development of good quality silicon wafers for applications in the new solid state electronics, that potentially useful quantities of power were produced by photovoltaic devices in crystalline silicon.

In the 1950s, the development of silicon electronics followed the discovery of a way to manufacture p-n junctions in silicon. Naturally n type silicon wafers developed a p type skin when exposed to the gas boron trichloride. Part of the skin could be etched away to give access to the n type layer beneath. These p-n junction structure produced mush better rectifying action than Schottky barriers, and better photovoltaic behaviors. The first silicon solar cell was reported by Chapin, Fuller and Pearson in 1954 and converted sunlight with an efficiency of 6%, six times higher than the best previous attempt. That figure was to rise significantly over the following years and decades but, at and estimated production cost of some 200 per Watt, these cells were not seriously considered for power generation for several decades. Nevertheless, the early silicon solar cell did introduce the possibility of power generation in remote locations where fuel could not easily be delivered. The obvious application was to satellites where the

requirement of reliability and low weight made the cost of the cells unimportant and during the 1950s and 60s, silicon solar cells were widely developed for applications in space.

Also in 1954, a cadmium sulphide p-n junction was produced with and efficiency of 6%. And in the following years studies of p-n junction photovoltaic devices in gallium arsenide, indium phosphide and cadmium telluride were stimulated by theoretical work indicating that these materials would offer a higher efficiency. However, silicon remained and remains the foremost photovoltaic material, benefiting from the advances of silicon technology for the microelectronics industry. Short histories of the solar cell are given elsewhere [Shive,1959; Wolf,1972; Green, 1990]

In the 1970s the crisis in energy supply experienced by the oil-dependent western world led to a sudden growth of interest in alternative sources of energy, and funding for research and development in those areas. Photovoltaic was a subject of intense interest during this period, and a range of strategies for producing photovoltaic devices and materials more cheaply and for improving device efficiency were explored. Routes to lower cost included photoelectrochemical junctions, and alternative materials such as photocrystalline silicon, amorphous silicon, other 'thin film' materials and organic conductors. Strategies for higher efficiency included tandem and other multiple band gap designs. Although none of these led to widespread commercial development, our understanding of the science of photovoltaic in mainly rooted in this period.

During the 1990s, interest in photovoltaic expanded, along with growing awareness of the need to secure sources of electricity alternative to fossil fuels. The trend coincides with the widespread dregulation of the electricity markets and growing recognition of the viability of decentralized power. During this period, the economics of photovoltaic improved primarily through economies of scale. In the late 1990s the photovoltaic production expanded at a rate of 15-25% per annum, driving a reduction in

cost. Photovoltaic first became competitive in contexts where conventional electricity supply is most expensive, for instance, for remote low power applications such as navigation, telecommunications, and rural electrification and for enhancement of supply in grid-connected loads at peak use [Anderson, 2001]. As prices fall, new markets are opened up. An important example is building integrated photovoltaic applications, where the cost of the photovoltaic system is offset by the savings in building materials.

2.2 Operating principles and structure of DSSC

2.2.1 Cell structure:

DSSC consists of three main components a dye-covered nanocrystalline TiO_2 layer on a transparent conductive glass substrate, an electrolyte contained iodide/ triiodide redox couple, and a platinized conductive glass substrate as a counter electrode (see Figure 2.1).
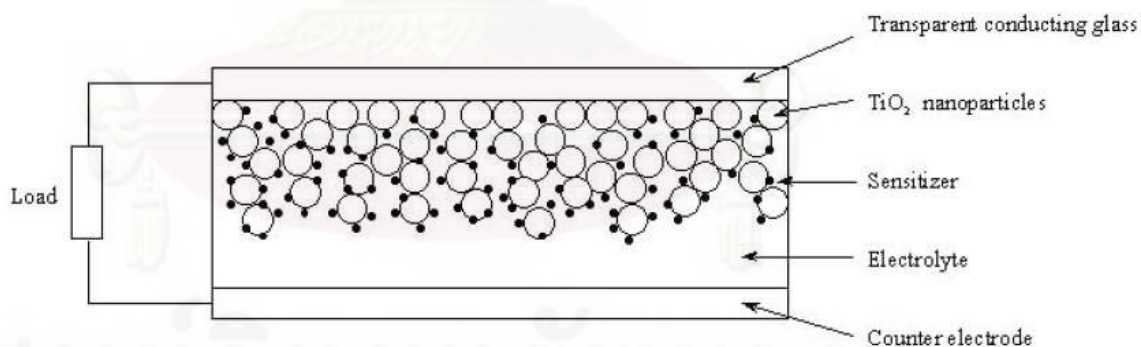
Figure 2.1: Structure of dye-sensitized solar cell

(Pongsaton Amornpitoksuk and Nararak Leesakul, 2003)

2.2.2 Operating Principles:

In detail, the operation of dye-sensitized solar cell can be described in schematic structure of DSSC shown in Figure 2.1.

1. Light absorption the dye molecule is excited from their ground state (S) to an excited state (S*).

2. The dye injects an electron into the conduction band (CB) of semi-conductor layer (TiO_2), leaving an oxidized dye (S^+).

3. The electrons pass through to the external circuit.

4. The electron donor present in the electrolyte reduces the oxidized dye (S^+) back to the ground state (S).

5. The iodide is regenerated, in turn, by reduction of triiodide at the counter electrode.

There are a number 6 and 7 of undesired pathways in this process. The electron in the conduction band can reduce the oxidized dye (S^+) or can regenerate the redox couple.
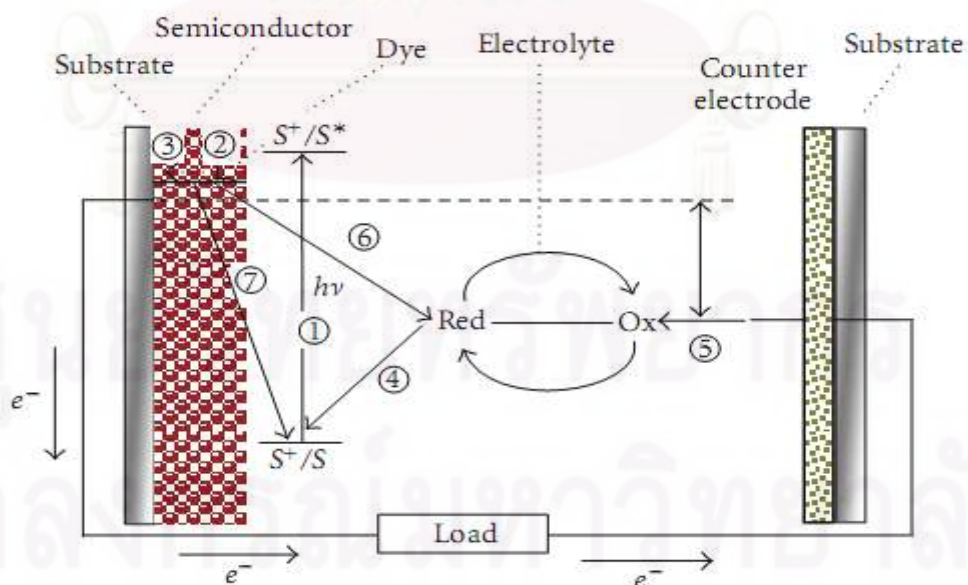
Figure 2.2: Operation principle of DSSC (Kong et al., 2007)

2.3 Characteristic of the Photovoltaic cell

2.3.1 Efficiency

There are several important measures that are used to characterize solar cells. All of these should be defined for particular illumination conditions. The cell power density is given by

$$P = IV \qquad (2.1)$$

Where

P = the power (watt or w)

I = the current (ampere or A)

V = potential difference (volt or v)

P reaches a maximum at the cell's operating point or maximum power point. This occurs at some voltage V_{mp} with a corresponding current density I_{mp}, shown in Figure.2.3. The optimum load thus has sheet resistance given by V_{mp}/I_{mp}. The fill factor is defined as the ratio

$$FF = \frac{I_{mp}V_{mp}}{I_{sc}V_{OC}} \qquad (2.2)$$

Where

I_{mp} = the current at maximum power

V_{mp} = potential difference at maximum power

FF = fill factor

I_{sc} = the short-circuit current

V_{OC} = the open-circuit voltage
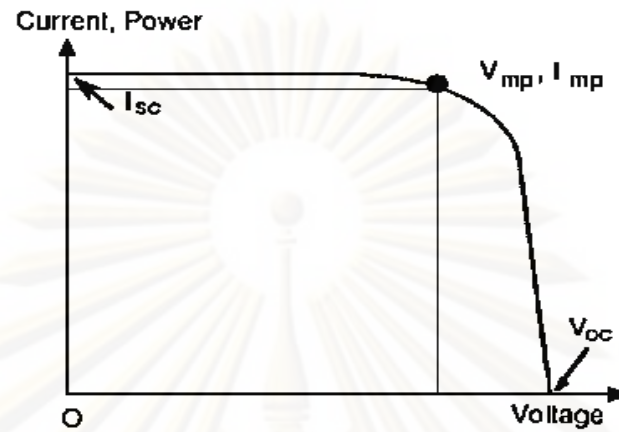
Figure 2.3: I-V characteristic of an illuminated solar cell

The efficiency (η) of the cell is the power density delivered at operating point as a fraction of the incident light power density, P_S,

$$\eta = \frac{I_{mp}V_{mp}}{P_S} \qquad (2.3)$$

Efficiency is related to I_{SC} and V_{OC} using FF,

$$\eta = \frac{I_{sc}V_{oc}FF}{P_S} \qquad (2.4)$$

Where

η = efficiency of solar cell

P_S = power of light source

2.4 Components of DSSC.

2.4.1 Dye sensitizer

Dye-sensitizer serves as the solar energy absorber in DSSC. Its proprieties have much effect on the light harvesting efficiency and the overall photoelectrical conversion efficiency. Three commonly-used dyes in DSSC consists of ruthenium based metal organic complexes. Their commercial names are N-3(Red dye), N-719(Black dye) and Z-907. This research was selected N-3 dye in Table 2.1 shown physicochemical properties of N-3. Figure 2.4 shows their chemical structures.

N-3   N-719

Z-907
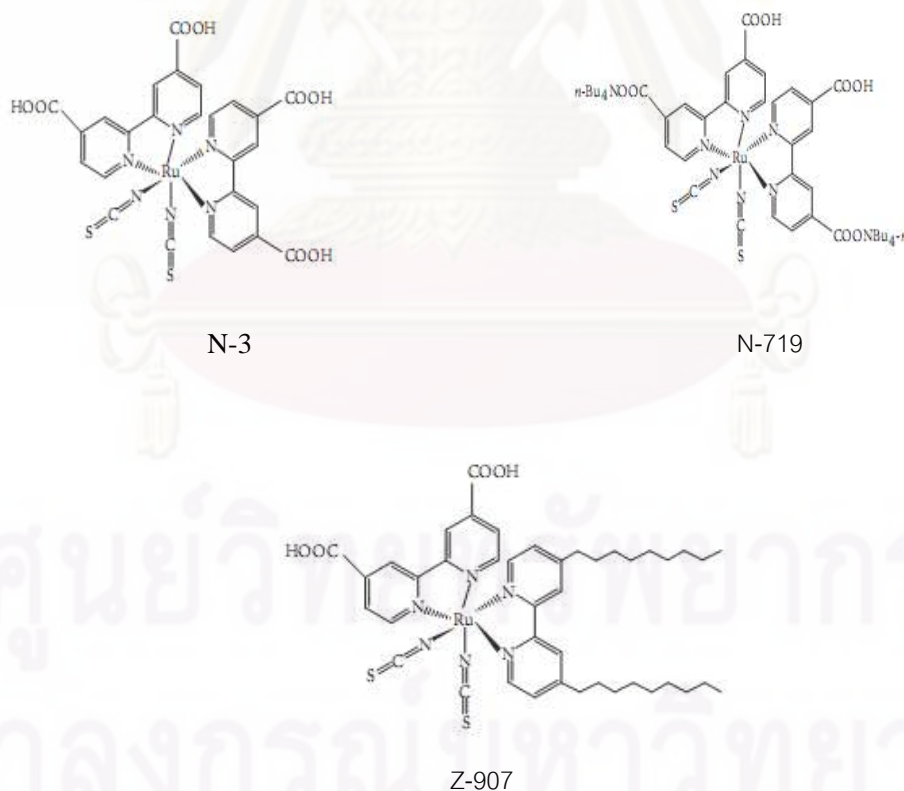
Figure 2.4 Molecular structures of three types of ruthenium dyes (Kong et al., 2007)

Table 2.1 Physicochemical properties of N-3.

Product designation:	Ruthenium 535 (also known as "N3")
Chemical Name:	*cis*-bis(isothiocyanato)bis(2,2'-bipyridyl-4,4'-dicarboxylato)-ruthenium(II)
Short Formula:	$RuL_2(NCS)_2.2H_2O$ (L = 2,2'-bipyridyl-4,4'-dicarboxylic acid)
Molecular Formula:	$C_{26}H_{20}O_{10}N_6S_2Ru$
Molecular Weight:	741.7 g/mol

2.4.2 Electrolyte

The electrolyte is one of the key components for dye-sensitized solar cells and its properties have much effect on the conversion efficiency and stability of the solar cells. Liquid electrolyte could be divided into organic solvent electrolyte and ionic liquid electrolyte, according to the solvent used.

Organic solvent electrolytes were widely used in dye-sensitized solar cells for their low viscosity, fast ion diffusion and high efficiency into nanocrystalline film electrode. The composition of the electrolytes includes organic solvent, redox couple, and additive.

Organic solvent used in organic liquid electrolyte includes nitrile such as acetonitrile, valeronitrile, and 3-methoxypropionitrile; and esters such as ethylene carbonate, propylene carbonate, and γ-butyrolactone.

The commonly used additive in the electrolytes for dye-sensitized solar cells contains 4-tert-butylpyridine (TBP) and N-methylbenzimidazole (NMBI). The addition of these additives suppresses the dark current and improves the photoelectric conversion efficiency. TBP also reduces the recombination of electrons in the conduction band of the semiconductor and the electron acceptor in the electrolyte through the coordination between the N atom and the Ti ion in an incomplete coordination state on the surface of TiO_2 film. Consequently, the photovoltage fill factor and the conversion efficiency increases dramatically.

The maximum efficiency record of DSSC was obtained by the solar cells based on organic solvent electrolyte, especially the highly volatile organic solvent electrolyte due to the efficient infiltration of organic electrolyte in nanocrystalline films. However, the solar cells based on organic electrolyte have the disadvantages such as bad long-term stability, difficulty in robust sealing and leakage of electrolyte due to the volatility of organic solvent.

2.5. Titanium Dioxide

2.5.1 The methods for synthesizing titanium dioxide

There are several methods that can be used to synthesize anatase titania. In general, the methods that have been reported for anatase synthesis are sol-gel method, chemical vapor deposition, thermal decomposition method, and precipitation method.

2.5.1.1. Sol-Gel method

This method can be performed at relatively low temperature. This method starts at mixing titanium alkoxide with alcohol. The mixture of water and acid was added to first mixture. The sol-gel was formed by hydrothermal process. This technique can be applicated by using ultrasonic spray coater to aid dispersion and the efficiency of titania with higher surface area, better thermal stability than stirring method.

The average crystal size of titania by this method were in the range of 4 – 8 nm and BET surface area were in the range of 91-120 m^2/g depend on calcination temperature. However the limits of this method are the strong reactivity of alkoxide toward H_2O often results in an uncontrolled precipitation.

Sol-gel process occurs in liquid solution of organometallic precursors (e.g., titanium isopropoxide), which lead to the formation of sol by means of hydrolysis and condensation reaction.

$$M\text{-}O\text{-}R \ + \ H_2O \qquad \Rightarrow \qquad M\text{-}OH \ + \ R\text{-}OH \qquad \text{hydrolysis} \qquad (2.5)$$

$$M\text{-}O\text{-}H \ + \ HO\text{-}M \qquad \Rightarrow \qquad M\text{-}O\text{-}M \ + \ H_2O \qquad \text{water condensation} \qquad (2.6)$$

$$M\text{-}O\text{-}R \ + \ HO\text{-}M \qquad \Rightarrow \qquad M\text{-}O\text{-}M \ + \ R\text{-}OH \qquad \text{alcohol condensation} \qquad (2.7)$$
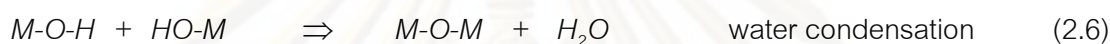
A typical example of a sol-gel method is the addition of metal alkoxide to water. The alkoxide is hydrolyzed, giving the oxide as a colloidal product.

The sol is made of solid particles of a diameter of few hundred nanometers suspended in a liquid phase. After that, the particles condense into gel, in which solid macromolecules are immersed in a liquid phase. Drying the gel at low temperature (25-100°C) produces porous solid matrices or xerogels. To obtain a final product, the gel is heated. This heat treatment serves several purposes, i.e., to remove solvent, to decompose anions such as alkoxides or carbonates to give oxides, to rearrange of the structure of the solid, and to allow crystallization to occur.

Using the sol-gel method, one can easily control a stoichiometry of solid solution and a homogeneous distribution of nanoparticles and metal oxides. In addition, the advantages are that the metal oxides are prepared easily at room temperature and high purity can be obtained.

2.5.1.2. Chemical Vapor Deposition

This method involves the formation of nanocrystalline titanium dioxide by hydrolysis and condensation of titanium alkoxide. The preparation is conducted in an aerosol reactor which is made of two concentric glass tubes that is externally heated in a vertical furnace. Titanium precursor is evaporated at different temperatures to obtain different vapor pressures and carried by nitrogen gas into the reactor. Water vapor is then introduced into the reactor by dry air. Precursor vapor and water vapor are mixed rapidly and react to form TiO_2 aerosol at atmospheric pressure. Consequently, the product is collected by thermophoresis and filter. The as-prepared TiO_2 powder is then put into furnace for heat treatment (Xia et al., 1999).

2.5.1.3. Thermal Decomposition method

This method has been used to successfully synthesize various types of nanosized metal oxides with large surface area, high crystallinity and high thermal stability (Payakgul et al., 2005). Titanium precursor (e.g., titanium alkoxide), is used as a starting material. The precursor is first suspended in organic solvent in a test tube inside an autoclave. The crystalline titania is formed at temperature in the range of 200-300 $^{\circ}$C in an autoclave. Autogeneous pressure during the reaction gradually increases as the temperature is raised. The physiochemical properties of the synthesized titania depend on the reaction conditions as well as the calcination temperature.

2.5.1.4. Precipitation method

Ultrafine crystalline TiO_2 powder is prepared by heating and stirring of aqueous $TiOCl_2$ solution with Ti^{4+} concentration of 0.5 mol/l at room temperature up to 100 $^{\circ}$C under normal atmospheric pressure (Nam et al., 1999). TiO_2 crystals in pure rutile phase precipitated at a temperature below 65 $^{\circ}$C. On the other hand, TiO_2 precipitates in crystalline anatase phase at a temperatures above 65°C. The direct

formation of TiO_2 crystalline precipitates from aqueous $TiOCl_2$ solution is a result of the existence of the hydroxide ions in water, which causes the crystallization of $TiOCl_2$ into TiO_2 without hydrolyzation to $Ti(OH)_4$. Conventionally, rutile-phase TiO_2 is synthesized at a much higher temperature.

2.5.2. Thickness of TiO_2 film

The commonly of coating TiO_2 on a glass have difference method are doctor blade, spray coating, spin coating, vapor deposition, screen printing and reactive sputtering. Halme and coworker (2006) studied the spray deposition of TiO_2 powder suspension at the room temperature compression as a method to prepare nanostructured TiO_2 films for dye-sensitized solar cell. Relatively good solar cell performance of a light intensity of 2.8% at 100 mW/cm^2 was achieved with the method. The critical point in the spray deposition method was the successful control of the evaporation rate of the suspension liquid with respect to the deposition rate.

Film thickness is one of the important factors. Thickness affects the performance of the cells because the injected electrons have to be transported across a large number of colloidal particles and grain boundaries. One study has shown that film thickness increased with the short-circuit photocurrent (I_{sc}) increased because of increasing the absorption of dye on TiO_2 surface (Kang et al., 2004).

However the thickness increases the chance of recombination should increase. Therefore, there exists an optimum film thickness to obtain a maximum photo-voltage and fill factor (Kalyanasundaram et al., 1998).

2.5.3. Physical and Chemical Properties (Fujishima et al., 1999)

Titanium dioxide may take on any of the following three crystal structures: anatase, which tends to be more stable at low temperature; brookite, which is usually found only in minerals; and rutile, which tends to be more stable at higher temperatures and thus is sometimes found in igneous rock.

Anatase generally shows a higher photocatalytic activity than the other types of titanium dioxide. Comparison of some physical properties of anatase, brookite and rutile is listed in Table 2.2.

Although anatase and rutile are both tetragonal, they do not have the same crystal structures. Anatase exists in near-regular octahedral structure and rutile forms slender prismatic crystal. Rutile is the thermally stable form and is one of the two most important ores of titanium.

The three forms of titanium (IV) oxide have been prepared in laboratories but only rutile, the thermally stable form, has been obtained in the form of transparent large single crystal. The transformation from anatase to rutile is accompanied by the evolution of ca. 12.6 kJ/mol (3.01 kcal/mol), but the rate of transformation is greatly affected by the presence of other substances, which may either catalyze or inhibit the reaction. The lowest temperature at which transformation from anatase to rutile takes place at a measurable rate is around 700°C, but this is not a transition temperature. The change is not reversible since ΔG for the change from anatase to rutile is always negative.

Table 2.2 Comparison of rutile, brookite and anatase. (Fujishima et al., 1999).

Properties	Anatase	Brookite	Rutile
Crystal structure	Tetragonal	Orthorhombic	Tetragonal
Optical	Uniaxial, negative	Biaxial, positive	Uniaxial, negative
Density, g/cm^3	3.9	4.0	4.23
Harness, Mohs scale	$5^1/_2 - 6$	$5^1/_2 - 6$	$7 - 7^1/_2$
Unit cell	$D_4a^{19}.4TiO_2$	$D_2h^{15}.8TiO_2$	$D_4h^{12}.3TiO_2$
Dimension, nm			
a	0.3758	0.9166	0.4584
b	-	0.5436	-
c	0.9514	0.5135	2.953
Refractive index	2.52	-	2.52
Permittivity	31	-	114
Melting point	changes to rutile at high temperature	-	1858° C

Brookite has been produced by heating amorphous titanium (IV) oxide, which is prepared from an alkyl titanate or sodium titanate, with sodium or potassium hydroxide in an autoclave at 200 to 600 $^{\circ}$C for several days. The important commercial forms of titanium dioxide are anatase and rutile, and they can readily be distinguished by X-ray diffractometry.

2.5.4. Applications of titanium dioxide

Titanium dioxide is one of the most basic materials in our daily life. Titanium dioxide has been used in paints, plastics, paper, inks, fibers, cosmetics, sunscreens and foodstuffs.

Naturally, the type of titanium dioxide that is used as a pigment is different from that used as a photocatalyst. Various applications in which research and development activities involving titanium dioxide have been investigated, such as fog-proof, anti-bacterial, anti-viral, fungicidal, anti-soiling, self-cleaning, deodorizing, air purification, anti-cancer, water treatment and water purification.

CHAPTER III

LITERATURE REVIEWS

This chapter presents the literature reviews for dye-sensitized solar cell (DSSC).

3.1. Modification of TiO_2 electrode of a dye-sensitized solar cell

Lee and coworkers (2008) investigated multi-layered TiO_2 nanostructured films that were fabricated to improve the light harvest efficiency of the dye-adsorbed TiO_2 electrode in dye-sensitized solar cells (DSSC) by light scattering. Three different structures of TiO_2 electrodes, with layers consisting of TiO_2 pastes with average diameters of 9, 20, and 300 nm, respectively, were fabricated and their photovoltaic effects on the DSSC devices were measured. By utilizing the multi-layered TiO_2 electrode constructed from the three different TiO_2 pastes, the overall power conversion efficiency of the DSSC devices in the PEG-based electrolyte was increased to 5.24% under irradiation of 100 mW/cm^2 at AM 1.5. The use of the light scattering layers resulted in an increase in both the I_{sc} value and fill factor, thus increasing the overall power conversion efficiency of the DSSC devices.

Lee and coworkers (2009) prepared three different structures of TiO_2 electrodes of the dye-sensitized solar cell (DSSC) with layers of nanoparticles and light-scattering particles, and their photovoltaic performances were investigated when the polymer electrolytes were used. Especially, 20-nm- and 123-nm-TiO_2 pastes were prepared by using sol–gel method, to use for light-scattering layer. The best efficiency of 6.03% was attained with a multi-layer structure using 123-nm-TiO_2 layer for the light-scattering layer and 9-nm-TiO_2 layer for the dense layer.

Koo and coworkers (2007) studied the effect of scattering particle size on light scattering efficiency in dye-sensitized solar cell with a FTO/semitransparent nano-TiO_2 layer (main-layer)/scattering layer (overlayer) structure, where two different rutile TiO_2 particles with a size of 0.3 μm (G1) and 0.5 μm (G2) were used for a scattering overlayer and 20-nm anatase particle for nano-TiO_2 main-layer. The conversion efficiency of 7.55% for the 7 μm-thick main-layer film was improved to 8.94% and 8.78% when G1 and G2 particulate overlayers were introduced, respectively, corresponding to 18.4% and 16.3% increases. While the conversion efficiency of the 14 μm-thick main-layer was slightly improved from 8.60% to 9.09% and 9.15% upon depositing G1 and G2 particulate overlayers, respectively. Therefore, scattering efficiency was significantly influenced by the reflectivity of the scattering overlayer, which was related to the size and refractive index of the scattering particles as well as the nanocrystalline film thickness used as a main layer.

Yu and coworkers (2009) prepared TiO_2 organic sol for the preparation of a compact TiO_2 layer on fluorine-doped tin oxide (FTO) glass by a dip-coating technique. The resultant thin film was used for the fabrication of dye-sensitized solar cells (DSSC). The compact layer typically had a thickness of ca. 110 nm as indicated by SEM and consisted of anatase as confirmed by the XRD pattern. Compared with the traditional DSSC without this compact layer, the solar energy-to-electricity conversion efficiency, short-circuit current and open-circuit potential of the DSSC with the compact layer were improved by 33.3%, 20.3%, and 10.2%, respectively.

Hossain and coworkers (2008) attempted to prevent short-circuits in the solar cells and back transfer of electrons due to direct contact between the electrolyte and the conductive substrate. A thin passivating TiO_2 under layer was deposited on SnO_2:F coated glass substrate by sputtering technique with different sputtering pressures of 0.1, 1.0 and 2.0 Pa. An upper nanoporous TiO_2 layer was deposited by conventional

sol–gel technique with 2.0 g of polyethylene glycol. The passivating layer that was deposited with 0.1 Pa sputtering pressure exhibited maximum efficiency.

Lee and coworkers (2006) prepared four different configuration for the coating of TiO_2 suspension, with low and high molecular weight poly(ethylene glycol) as a binder. Among these four systems, P2P1, where P1 and P2 correspond to the molecular weight of PEG of 20,000 and 200,000 respectively, showed the highest efficiency. The best efficiency (η) was 9.04% with the short-circuit photocurrent density (I_{sc}) and open-circuit voltage (V_{oc}) of 18.9 mA/cm^2 and 0.74 V, respectively.

Chang and coworkers (2010) coated Degussa P25 on an indium tin oxide (ITO) glass substrate by electrophoresis deposition. The coated glass was combined with N719 dye, an electrolyte solution and a counter-electrode of Pt layer to produce dye-sensitized solar cells (DSSC). In this process, the thickness of a single TiO_2 film was approximately 3.3 μm. Stacking was then performed to obtain a multilayer-typed TiO_2 film of ca.12 μm thick. As the sintering temperature reached 400°C, the prepared multilayer TiO_2 film increased the dye adsorption of the thin film and enhanced its adsorption percentage. The I–V curve of the produced DSSC showed that it had an excellent energy conversion efficiency of 6.9%.

Xu and coworkers (2010) fabricated bilayer-structured film with TiO_2 nanocrystals as underlayer and TiO_2 nanotubes as overlayer. The resulting double-layer TiO_2 (DL-TiO_2) film significantly improved the efficiency of dye-sensitized solar cells. The overall energy-conversion efficiency (η) of 6.15% was achieved by the formation of DL-TiO_2 film, which was 44.7% higher than that formed by pure nanocrystalline TiO_2 film and far larger than that formed by nanotube TiO_2 film.

3.2 Effect of thickness and sintering temperature for TiO_2 film on efficiency of dye-sensitized solar cell

Huang and coworkers (2006) studied the effect of hydrothermal temperature on the properties of TiO_2 colloids, and the effects of film thickness on the performance of a DSSC. With an increase in hydrothermal temperature, the pore diameter increased linearly. However, the surface area showed the reverse effect. The DSSC assembled with the TiO_2 films prepared under the hydrothermal temperature of 240 °C with the thickness larger than 10 mm gave optimal performance. The effect of film thickness of TiO_2 on the performance of the DSSC could be explained by the relative size of reactive species diffusing into the thin film and the lifetime of injected electrons.

Kao and coworker (2009) fabricated anatase TiO_2 thin films with different thicknesses (0.5–2.0 μm) have been deposited on ITO-coated glass substrates by a sol-gel method and rapid thermal annealing for application as the work electrode for dye-sensitized solar cells. From the results, the increases in thickness of TiO_2 films can Increase adsorption of the N3 dye through TiO_2 layers to improve the short-circuit photocurrent and open-circuit voltage.

CHAPTER IV

EXPERIMENTAL

The organization of this chapter is as follows: preparation of TiO_2 sol, preparation of dye-sensitized solar cell, fabrication of dye-sensitized solar cell components and the fabrication procedure, and characterization techniques employed in this study.

4.1 Preparation of TiO_2 sol

TiO_2 was prepared using a sol-gel method. Typically, a solution consisted of 14.44 ml of 70% nitric acid and 2000 ml of distilled water was prepared. Titanium (IV) isopropoxide in the amount of 166.80 ml was added slowly to the solution while being stirred continuously at room temperature. The mixture was stirred for 3-4 days until clear sol was obtained. Next, the clear sol underwent dialysis in a cellulose membrane. The distilled water used for dialysis was changed daily until a pH of 3.5 was obtained. The resulting TiO_2 sol was kept in a refrigerator until needed.

4.2 Preparation of dye-sensitized solar cell components and the fabrication procedure

This section discusses preparation of components in dye-sensitized solar cell (DSSC) and the fabrication procedure for DSSC. The components of DSSC are conducting glass, counter electrode, electrolyte, TiO_2 electrode, dye, and sealing material.

4.2.1 Transparent conducting glass

The conducting glass is a transparent glass coated with fluorine-doped tin oxide (FTO). The glass was purchased from Solaronix (Switzerland) under the commercial name TCO22-15. The conducting side of the conducting glass was identified by using a

multimeter. The conducting side had a sheet resistance of 15-20 ohm. The glass was cleaned with ethanol and dried before use.

4.2.2 Dye

In our research, we employed a widely-used N3 (R535) dye or cis-bis(isothiocyanato)bis(2,2'-bipyridyl-4,4'-dicarboxylato)-ruthenium(II), which was purchased from solaronix. To prepare the dye solution, 20 mg of N3 dye was dissolved in 100 ml of ethanol and the mixture was stirred until a homogeneous solution was obtained. The resulting product is a solution of 0.3 mM N3 dye in ethanol.

4.2.3 Electrolyte

Electrolyte consisted of 0.5 M lithium iodine (LiI), 0.05 M iodide (I_2), and 0.5 M 4-tert-butylpyridine (TBP) in acetronitrile. To prepare electrolyte , we mixed 2 g of LiI, 0.38 g of I_2, and 2.20 ml of TBP in 30 ml of acetronitrile. The solution was stirred untill homogeneity was obtained.

4.2.4 Platinum counter electrode

The counter electrode for the DSSC is platinum film coated on conducting glass. A platinum counter electrode was prepared by ion sputtering. A conducting glass was to rectangular piece that was 1.0 x 1.5 cm^2. The surface of the glass was cleaned with ethanol and dried. Masking tape was placed on one side of the glass as shown in Figure 4.1. Then platinum was sputtered on the conducting glass using ion sputterer (JEOL JFC-1100E) at 10 mA of ion current for four minutes. After sputtering, masking tape was removed.
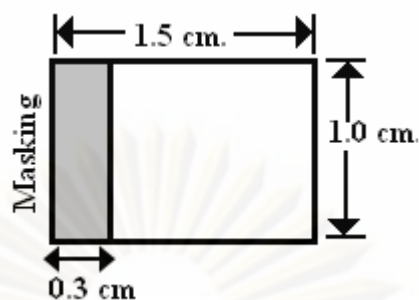
Figure 4.1 Schematic diagram of a platinum counter electrode

4.2.5 TiO$_2$ electrode

Anode electrode was a TiO$_2$ film on a conducting glass. To prepare the electrode, we first cut a conducting glass into a rectangular piece that was 1.0 cm wide and 1.5 cm long. The glass was cleaned with ethanol and dried. Then the glass was masked with aluminum foil containing a hole with a radius of 0.25 cm as shown in Figure 4.2 The hole was located closer to one side of the foil than the other.
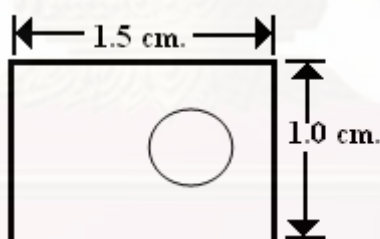
Figure 4.2 Aluminum foil used in preparation of an anode electrode before spray coating.

After masking, TiO$_2$ was coated on the conducting glass using ultrasonic spay coater. The TiO$_2$ sol was stirred, not shaken before use so as not to form bubbles. The spaying liquid was placed in a syringe pump, which fed the liquid at a rate of 1 ml/min to an ultrasonic nozzle.

The film thickness was varied by changing the number of coats of TiO_2 ranging from 200 to 500 coats. After a few coats, TiO_2 film was dried by a blow dryer. [The thickness of film was measured using a step profiler (Veeco Dektak 150)]. The coated glasses were sintered at a temperature ranging from $300^{\circ}C$ to $600^{\circ}C$ for two hours. After that electrode were left to cool down to $30^{\circ}C$. Before dye absorption, the electrode was heated on a hotplate at $70^{\circ}C$ for ten minute to remove water. The TiO_2 thin film electrode was immersed in solution of 0.3mM N3 dye overnight in the dark.

4.2.6 Fabrication of dye-sensitized solar cell assembly

Fabrication of dye-sensitized solar cell assembly started with cutting two strips of a sealing material (SX1170-25 is a 25 microns thick thermoplast hot-melt sealing foil) that were 0.15 cm wide and 1.2 cm long. The strips were inserted as spacers between the platinum counter electrode and TiO_2 electrode. The platinum counter electrode was placed on top of the TiO_2 electrode so that the conducting side of the counter electrode was on top of the TiO_2 film. The cell was sealed by heating the sealing material on a hotplate at $60^{\circ}C$ for three minutes. (see Figure 4.3)
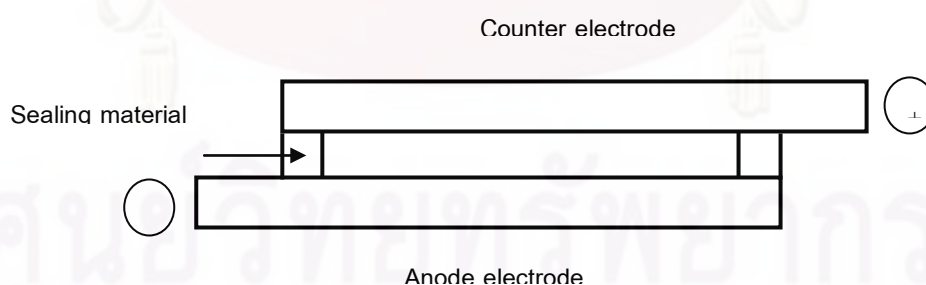
Figure 4.3 Cross-section of assembled dye solar cell showing sealing rim

After the anode and the counter electrode were attached together by the sealing material, electrolyte solution was injected between the two glass plates. Figure 4.4

displays an arrangement of various layers within a DSSC assembly, which is ready for testing.
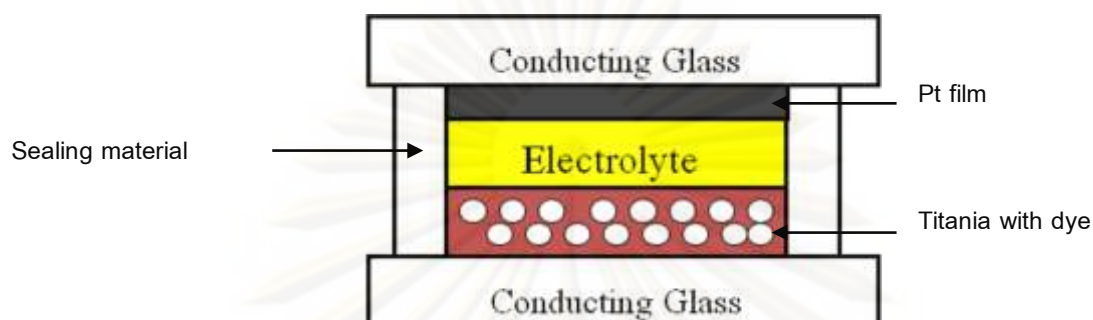
Figure 4.4 Fabrication of dye-sensitized solar cell assembly for testing

4.3 Physical and Electrochemical Characterization

In order to determine physical and electrochemical properties of TiO_2 and DSSC, various characterization techniques were employed. Such techniques are discussed in this section.

4.3.1 X-ray diffractometry (XRD)

XRD was performed to determine crystal phase and crystallite size of TiO_2. The characterization was conducted using a SIEMENS D5000 X-ray diffractometer with CuK_α radiation (λ = 1.54439 A$^\circ$) with Ni filter. The spectra were scanned at a rate of 0.04 min^{-1} in the 2θ range of 20-80°.

4.3.2 Nitrogen physisorption

Specific surface area of TiO_2 was measured through nitrogen gas adsorption in a continuous flow method at liquid nitrogen temperature. A mixture of nitrogen and helium was employed as the carrier gas using Micromeritics ChemiSorb 2750 Pulse

Chemisorption System instrument. The sample was thermally treated at 200°C for one hour before measurement.

4.3.3 UV-Visible Absorption Spectroscopy (UV-Vis)

The amount of dye adsorption was determined by a spectroscopic method by measuring the concentration of dye desorbed on the titania film into a mixed solution of 0.1 M NaOH and ethanol (1:1 in volume fraction). The absorption spectra were measured by a Perkin Elmer Lampda 650 with a scanning range between of 300-800 nm

4.3.4 Step profilmeter

The thickness of TiO_2 film obtained was measured by step profiler Veeco Dektak 150.

4.3.5 Photoluminescence (PL)

To study the recombination of electrons-holes, photoluminescence measurement was carried out on a Perkin-Elmer LS-55 fluorescence spectrophotometer by using a Xenon lamp as the excitation source at room temperature and excitation wavelength used in photo luminescence (PL) measurement was 300 nm.

4.3.6 Current-Voltage Tester (I-V Tester)

The electrochemical properties of dye-sensitized solar cell were determined by I-V tester Current–voltage measurements were performed using white light source under air mass (AM) 1.5G conditions. The current density, open circuit voltage, cell resistance, and fill factor were measured and were then converted to efficiency of the solar cell. An area of our solar cell was 0.196 cm^2. The equipment used was MV Systems Inc., Xenon short ARC (Osram XBO 1000 W/HS)

CHAPTER V

RESULTS AND DISSCUSSION

The result and discussion in this chapter are dividing into three parts, namely, effect of sintering temperature, effect of thickness of TiO_2 electrode layer for single-layer and double-layer TiO_2 films on the performance of dye-sensitized solar cell.

5.1 Dye-sensitized solar cell using single-layered conducting glass

5.1.1 Effect of sintering temperature for TiO_2 electrode

TiO_2 sol was prepared via sol-gel method and was used to make anode electrode in DSSC. Sintering temperature of TiO_2 could affect on specific surface area, crystallite size. These properties had influence on efficiency of dye-sensitized solar cell. In this work, the sintering temperature was to be varied 300 $^{\circ}$C, 400 $^{\circ}$C, 500 $^{\circ}$C and 600 $^{\circ}$C for 2 hours.

The XRD pattern of various titanium dioxide samples in the 2θ range between 20° and 80° are shown in Figure 5.1. The typical X-ray diffraction patterns of TiO_2 films sintered at various temperatures. The anatase phase of TiO_2 started to forms at a sintering temperature of 300 $^{\circ}$C. When the sintering temperature reached 600 $^{\circ}$C, the rutile phase became the major component. Small amount of brookite was detected in all samples.

The average crystallite size of anatase was estimated from the half-height width of (101) diffraction peaks. Crystallite size of anatase (as determined by Debye-Scherrer's equation) grew from 5.6 nm to 18.2 nm as sintering temperature was raised from 300 °C to 600 °C. The weight fraction of rutile phase of TiO_2 increased while the

weight fraction of anatase. Next, we determined specific surface area of TiO_2 powder from nitrogen adsorption technique.The result are presented the specific surface area of TiO_2 that decreased with increasing sintering temperature (see Table 5.1 and 5.2).
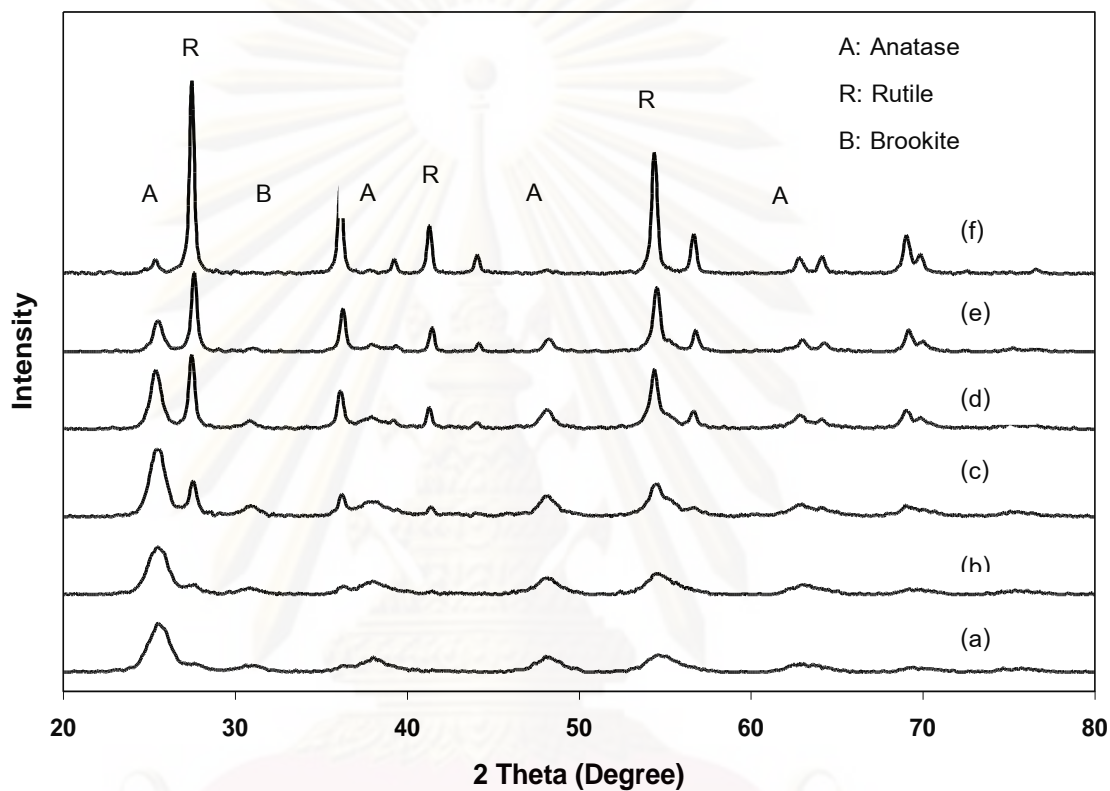
Figure 5.1 XRD pattern of TiO_2 powders sintered at, (a) $300^{\circ}C$, (b) $350^{\circ}C$, (c) $400^{\circ}C$, (d) $500\,^{\circ}C$, (e) $550^{\circ}C$, and (f) $600^{\circ}C$

Table 5.1 Crystallite size and weight fraction of anatase, rutile and brookite phases of TiO$_2$ powders sintered at various temperatures

Sintering Temperature (°C)	Crystallite size (nm)	W_A	W_R	W_B
300	5.6	0.62	0.22	0.16
350	6.7	0.60	0.26	0.14
400	7.6	0.50	0.37	0.13
500	10.1	0.44	0.47	0.09
550	13.3	0.29	0.66	0.05
600	18.2	0.09	0.90	0.01

W_A : weight fraction of anatase phase.

W_R : weight fraction of rutile phase.

W_B : weight fraction of brookite phase.

Table 5.2 Specific surface area of TiO$_2$ powders sintered at various temperatures.

Sintering Temperature (°C)	Surface area (m^2/g)
300	118.4
350	101.3
400	86.3
500	61.9
550	35.6
600	25.4

The increasing of particle size can be attributed of crystallization of the surface amorphous structure and the connection of those small nanoparticles at higher sintering temperature are important for help electron transport of TiO_2 film electrode (Zhoa et al., 2008).

For this study, the electrode consisted of 400 coats of TiO_2 have film thickness was approximately 7.3 µm at various sintering temperature is shown in Figure 5.2. It was found that an increase in the sintering temperature decreased the amount of adsorbed dye onto the TiO_2 electrodes.
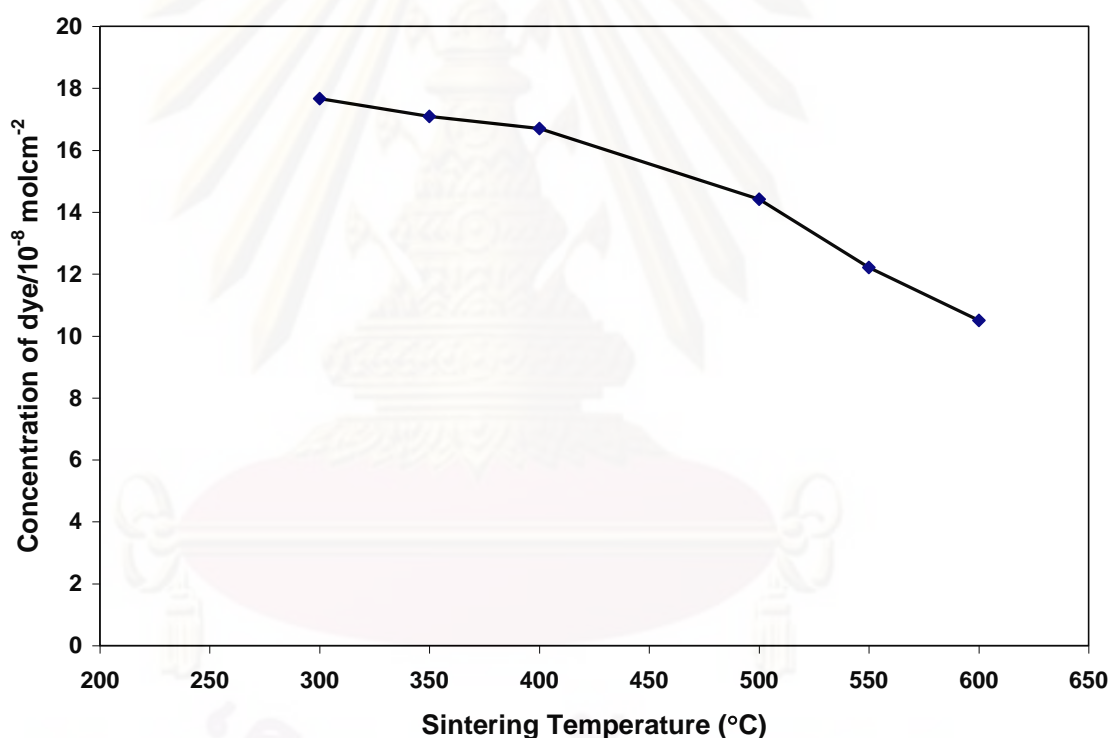
Figure 5.2 Relationship between concentrations of dye ang sintering temperature with film thickness about 7.3 µm

The PL measurement was carried out on a Fluorescence spectrophotometer (Perkin-Elmer LS-55). The PL signals of semiconductor materials result from the recombination of photo-induced charge carriers.The PL spectra of TiO_2 sintered at various temperatures were shown in Figure 5.3. It can be seen that the PL intensity of TiO_2 decreased as the sintering temperature increased. These results suggested that

the recombination rate of photogenerated electron and hole decreased when the sintering temperature increase, resulting in an increase of particle size (Liqiang et al., 2006 and Zhao et al., 2008).
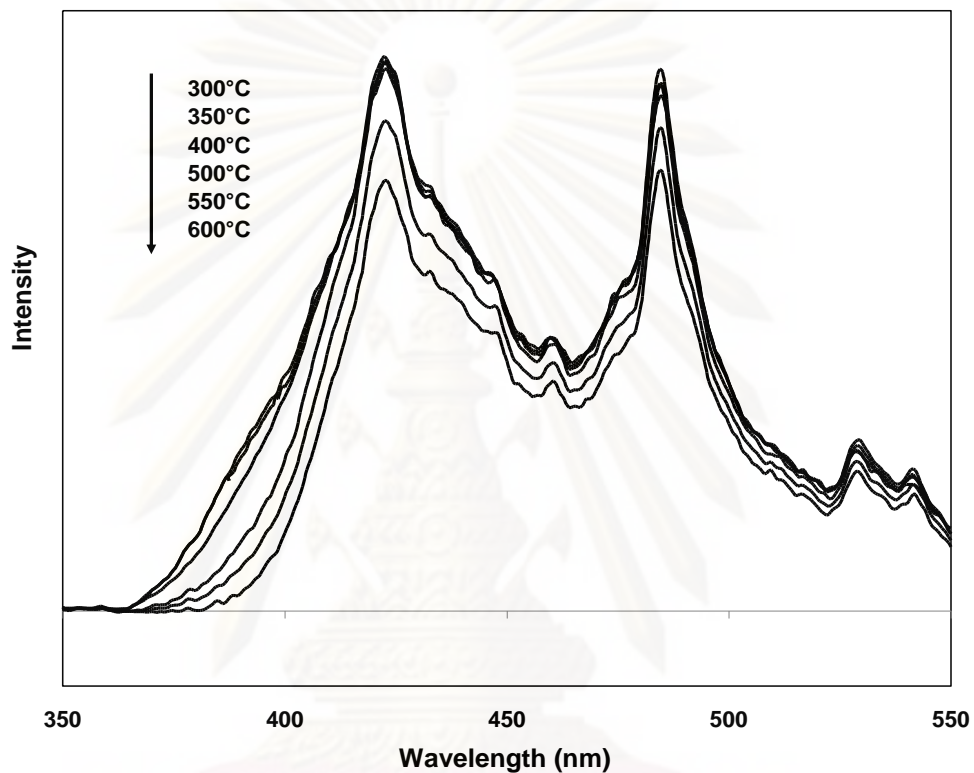
Figure 5.3 Photoluminescence spectra of TiO_2 sintered at various temperatures

The photovoltaic parameters of DSSC with a TiO_2 electrode that was calcined at various temperature are summerized in Table 5.3. The film thickness was about 7.31 μm at various sintering temperature for 2 h, this table show short-circuit current density (I_{SC}), open-circuit voltage (Voc), fill factor (FF) and cell efficiency (η) of DSSC.

We observed a maximum of short-circuit current density (I_{SC}) with a DSSC with a TiO_2 electrode calcined at 400 °C for two hours. Similar trend was observed in fill factor and cell efficiency. The efficiency of cell sintered at 500 °C and 600 °C decreases (see in Figure 5.4) because of the increasing of rutile phase (see in Table 5.1) leading to large particle size, less of surface area which due to absorption of dyes not enough.

Table 5.3 Photovoltaic parameters of DSSC with TiO_2 electrode sintered at various temperatures. The film thickness was about 7.31 μm.

Sintering Temperature (°C)	V_{OC} (Volt)	I_{SC} (mA/cm^2)	Fill Factor	*Efficiency (%)
300	0.71	3.43	0.69	1.68
350	0.71	3.71	0.74	1.94
400	0.74	4.44	0.82	2.69
500	0.71	3.92	0.77	2.14
550	0.69	3.79	0.75	1.96
600	0.68	3.58	0.73	1.80

*All values are average of two cells.
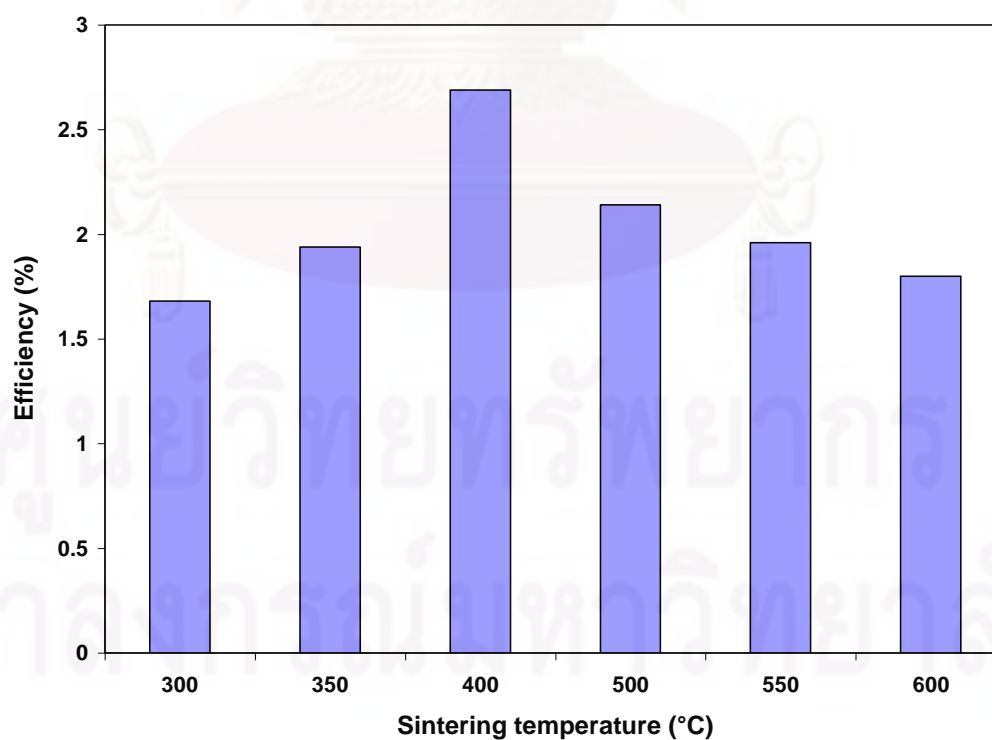
Figure 5.4 Efficiency of DSSC of TiO_2 at calcined at different temperature

5.1.2 Effect of thickness of TiO_2 film

We varied the thickness of TiO_2 electrode layer by varying number of coats of TiO_2 on the substrate. The numbers of coats of TiO_2 for this study were 200, 300, 400 and 500 coats. After coating, the electrode was sintered at 400 $^{\circ}$C for two hours. The film thickness was measured using step profilemeter.

From Figure 5.5 found that concentration of dye on TiO_2 surface increases with thickness of film increase because of increasing of the film thickness leading to increasing surface area of TiO_2 electrode (Kang et al., 2004).
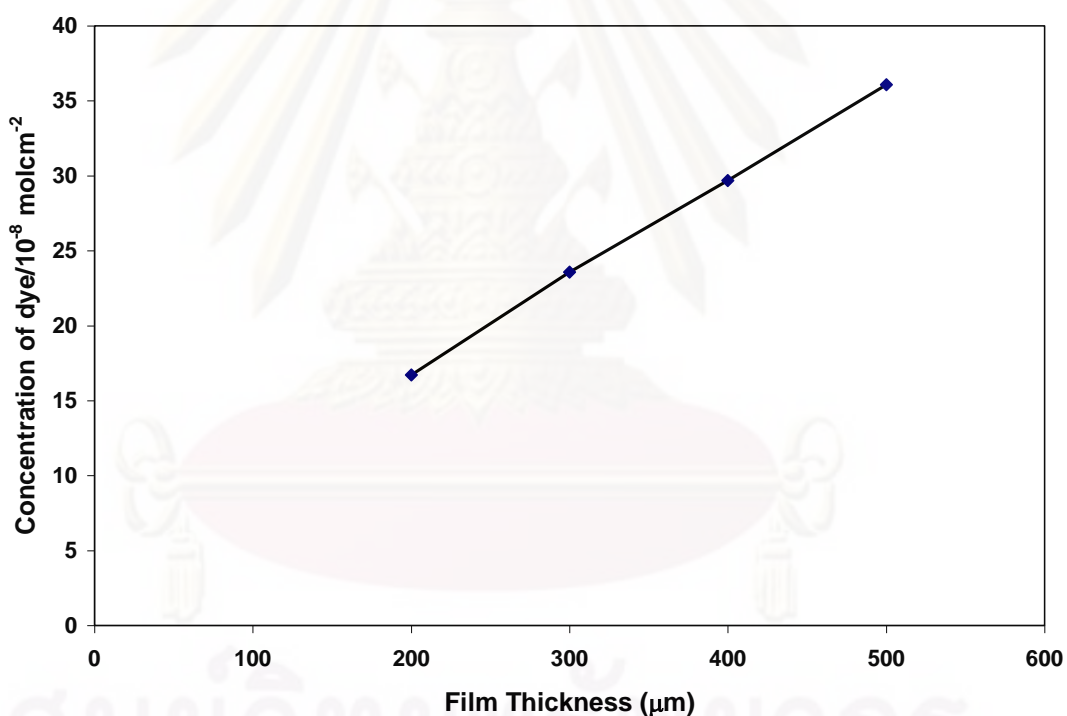
Figure 5.5 Relationship between concentrations of dye with various thickness of TiO_2 film at 400 $^{\circ}$C

The electrochemical properties of dye-sensitized solar cell of TiO_2 are listed in Table 5.4, this table show that the highest cell efficiency of 3.06% were observed in a DSSC with the thickest TiO_2 electrode layer (ca. 11 μm). The cell efficiency increased as the TiO_2 film thickness increased.

Table 5.4 Photovoltaic parameters of DSSC with TiO_2 electrode sintered at 400 $^{\circ}$C for two hours.

Film Thickness (µm)	V_{OC} (Volt)	I_{SC} (mA/cm^2)	Fill Factor	Efficiency (%)
3.68	0.73	3.51	0.71	1.82
5.57	0.76	4.02	0.75	2.29
7.31	0.74	4.44	0.82	2.69
11.19	0.72	4.83	0.88	3.06

From Figure 5.6, the efficiency of a DSSC increased from 1.82% to 3.06% when the number of coats of TiO_2 was increased from 200 to 500. The cell efficiency increases linearly with the thickness increases. The efficiency of cell at various sintering temperature and various film thickness (see Figure 5.7) described that increasing of film thickness, increasing of the efficiency of TiO_2 electrode for every sintering temperature. Figure 5.8 showed the UV–visible transmittance spectra of the TiO_2 films with different thicknesses between 300 and 900 nm in wavelength. It can be seen that all films have high transmittance. In addition, the transmittance of the films was lower as the films thicker.
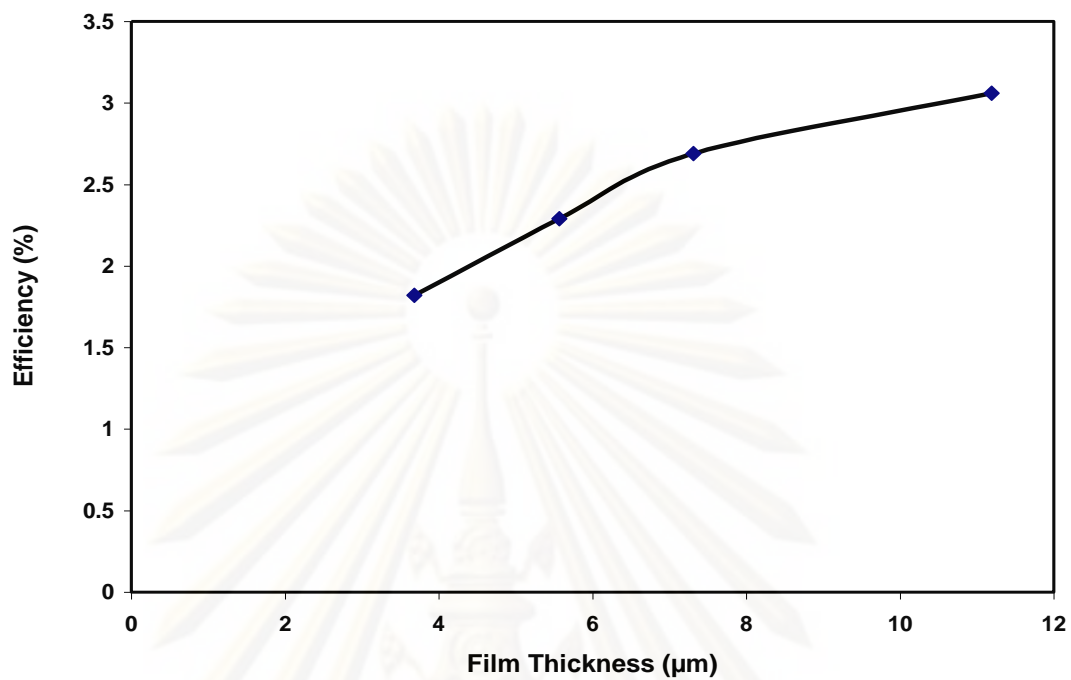
Figure 5.6 Efficiency of DSSC as a function of film thickness
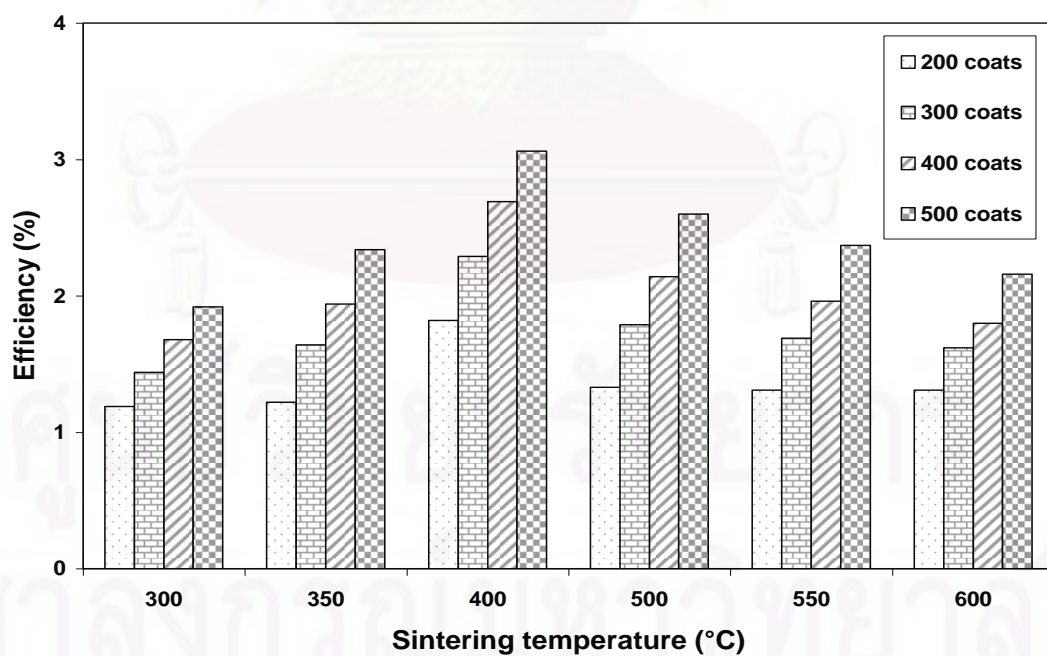
Figure 5.7 Efficiency of DSSC as a film thickness and sintering temperature of single-layered TiO_2 electrode
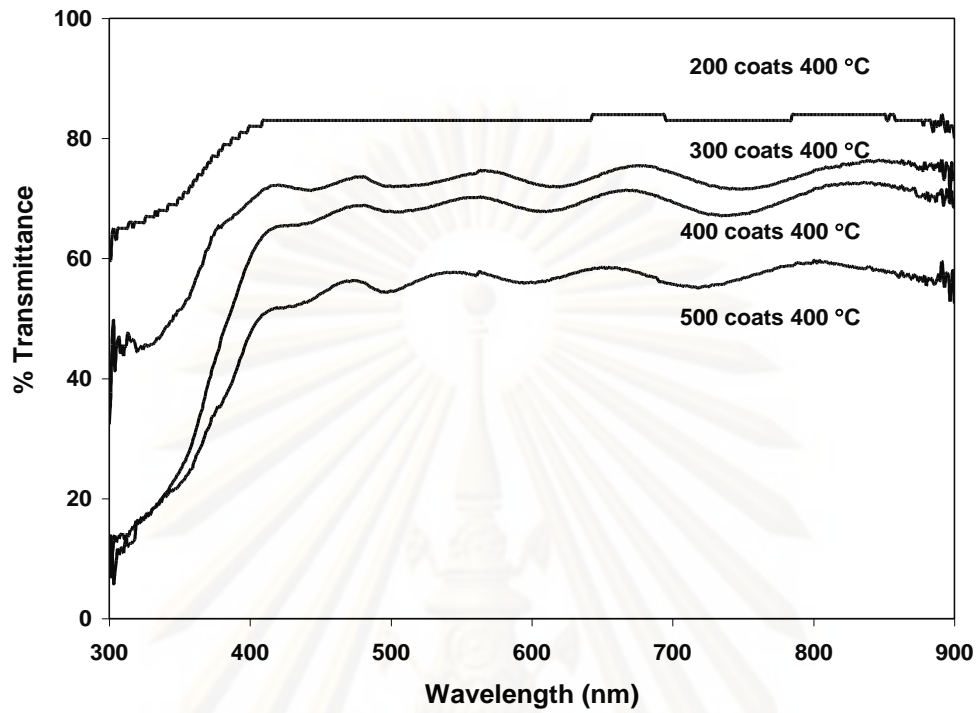
Figure 5.8 transmittance spectra of TiO$_2$ films with film thicknesses of 200 coats, 300 coats, 400 coats and 500 coats

5.2 Dye-sensitized solar cell using double-layered conducting glass

TiO_2 electrode was deposited onto conducting glass by the layer-by-layer deposition of double-layered TiO_2 particles. The bottom layer was coated on conducting glasses by using the ultrasonic spray coater. The film thickness was varied by changing number of coats of TiO_2 at 100, 150, 200 and 250. After deposition, TiO_2 film was dried by a hair dryer and then sintered at a temperature ranging from 300 $^\circ$C to 600 $^\circ$C for two hours.

Type A: Deposition TiO_2 sol on a conducting glass and then sintered at 350 $^\circ$C for two hour. Next, the deposition process was to obtain the desired film thickness same single-layer TiO_2 film. The TiO_2 films were finally sintered at a temperature 300°C for 15 minutes.

Type B: Deposition TiO_2 sol on a conducting glass and then sintered at 400 $^\circ$C for two hour. Next, the deposition process was to obtain the desired film thickness same single-layer TiO_2 film. The TiO_2 films were finally sintered at a temperature 350°C for 15 minutes.

Type C: Deposition TiO_2 sol on a conducting glass and then sintered at 600 $^\circ$C for two hour. Next, the deposition process was to obtain the desired film thickness same single-layer TiO_2 film. The TiO_2 films were finally sintered at a temperature 550°C for 15 minutes.

The TiO_2 of three types were immersed in 0.3 mM N3 dye for overnight in the dark. Structures A and B and C as a double-layer and shown in Figure 5.9.

300 15 min	350 15 min	550 15 min
350 2h	400 2h	600 2h
Conducting glass	Conducting glass	Conducting glass

| A type | B type | C type |
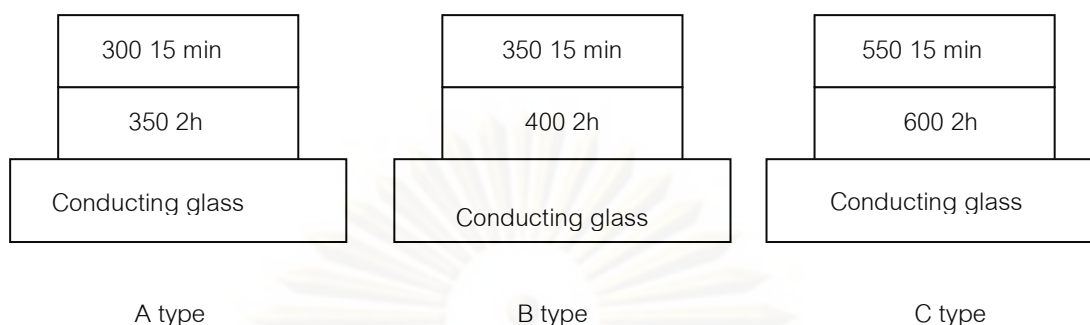
Figure 5.9 Three different types of TiO_2 electrode on conducting glass prepared for DSSC

5.2.1 Effect of sintering temperature for TiO_2 electrode

Double-layered TiO_2 electrode was $350^{\circ}C$ 2h and $300^{\circ}C$ 15 min, $400^{\circ}C$ 2h and $350^{\circ}C$ 15 min, $600^{\circ}C$ 2h and $550^{\circ}C$ 15 min.

The results from XRD analysis of TiO_2 powder (single-layered, double-layered) calcined at different temperature shown in Figure 5.10.

Figure 5.10 showed the XRD pattern at 2θ values of 25.32°, 37.88°, 48.16° and 62.80° corresponded to the anatase phase, whereas the XRD peak at 2θ values of 27.44°, 41.28° and 54.36° belonged to rutile phase and XRD peak at 30.88° belonged to brookite phase. The results are crystallite size, weight fraction of anatase, rutile and brookite phase presented in Table 5.5.

Crystallite size of double-layered less than single-layered. The crystallite sizes, calculated from the figure 5.10 using the peak 25.32° (anatase phase), are 6.3, 7.4 and 16.3 nm for double-layered TiO_2 film of $350^{\circ}C$ 2h and $300^{\circ}C$ 15 min, $400^{\circ}C$ 2h and $350^{\circ}C$ 15 min, $600^{\circ}C$ 2h and $550^{\circ}C$ 15 min, respectively. Next, we determined specific surface area of TiO_2 powders from nitrogen adsorption technique (see Table 5.6).
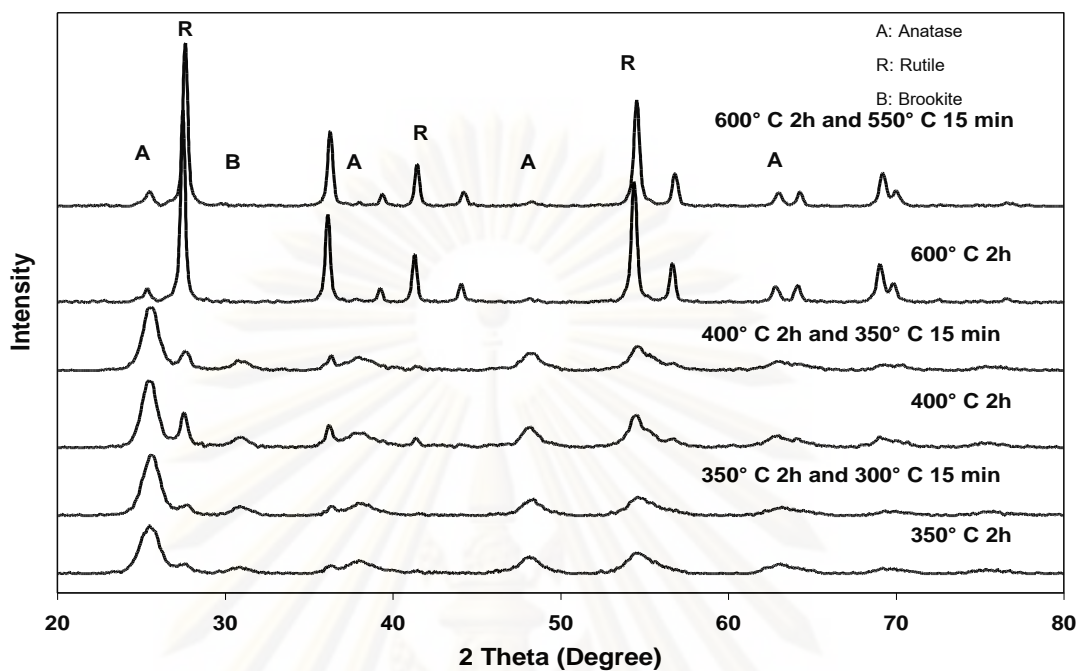
Figure 5.10 XRD pattern of TiO$_2$ powders sintered at different temperature

Table 5.5 Crystallite size and weight fraction of anatase, rutile and brookite phases of TiO$_2$ powders sintered at various temperatures

Sintering Temperature (°C)	Crystallite size (nm)	W_A	W_R	W_B
350°C 2h and 300°C 15 min	6.3	0.60	0.20	0.20
350°C 2h	6.7	0.60	0.26	0.14
400°C 2h and 350°C 15 min	7.4	0.57	0.26	0.17
400°C 2h	7.6	0.50	0.37	0.13
600°C 2h and 550°C 15 min	16.3	0.13	0.86	0.01
550°C 2h	13.3	0.29	0.66	0.05

W_A : weight fraction of anatase phase.

W_R : weight fraction of rutile phase.

W_B : weight fraction of brookite phase.

Table 5.6 Specific surface area of TiO_2 powders sintered at various temperatures.

Sintering Temperature (°C)	Surface area (m²/g)
350°C 2h and 300°C 15 min	97.31
350°C 2h	101.3
400°C 2h and 350°C 15 min	83.78
400°C 2h	86.3
600°C 2h and 550°C 15 min	35.99
550°C 2h	35.6

Table 5.7 displays the photovoltaic parameters of DSSC (single-layered TiO_2 electrode and double-layered TiO_2 electrode). The film thickness was about 7.31 µm at various sintering temperature for 2 h, this table show short-circuit current density (I_{SC}), open-circuit voltage (Voc), fill factor (FF) and cell efficiency (η) of DSSC

We compared photovoltaic parameters of single-layered TiO_2 electrode and double-layered TiO_2 electrode at nearly specific surface area, in which the thickness of single-layered TiO_2 electrode was experimentally controlled to be identical to that of double-layered TiO_2 electrode (ca. 7.31 µm). The DSSC with the double-layered TiO_2 electrode of 400°C 2h and 350°C 15 min shows the maximun efficiency, η(3.18%) and short-circuit current density, I_{SC}(4. 79) and open-circuit voltage (0.80 mV). All the DSSC with double-layer show higher efficiency than the DSSC with single-layer TiO_2 electrode.

Figure 5.11 represents the diffused reflection spectra of single-layered and double-layer TiO_2 electrode. The diffused reflectance of the films increases as the scattering layers were added.
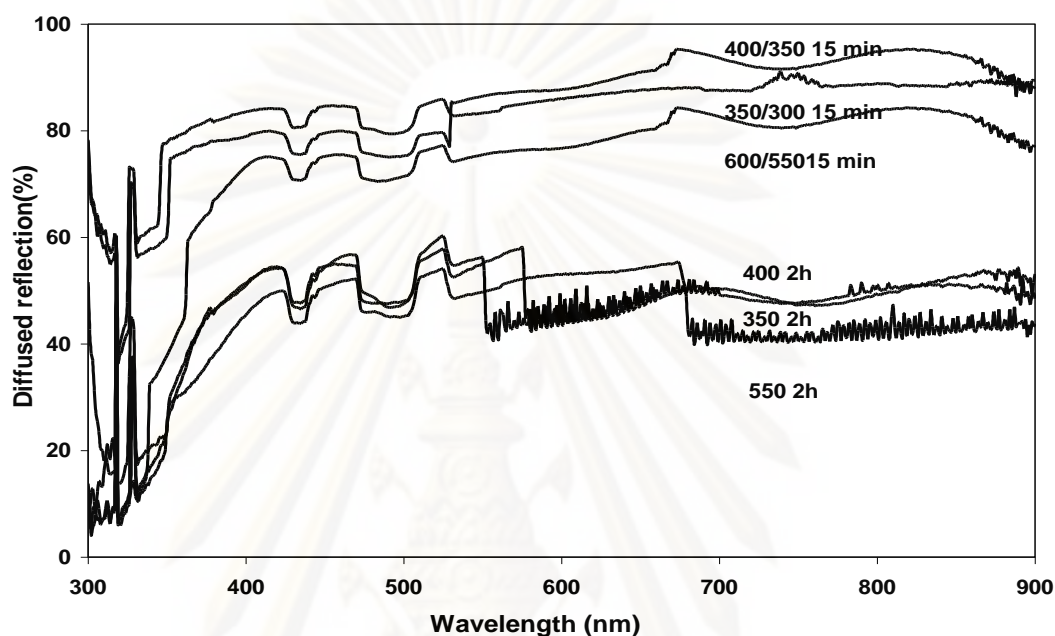
Figure 5.11 Diffused reflection of single-layered and double-layered

Table 5.7 Photovoltaic parameters of DSSC with TiO_2 electrode sintered at various temperatures. The film thickness was about 7.31 μm.

Sintering Temperature (°C)	V_{OC} (Volt)	I_{SC} (mA/cm^2)	Fill Factor	Efficiency (%)
350°C 2h and 300°C 15 min	0.79	4.64	0.82	3.01
400°C 2h and 350°C 15 min	0.80	4. 79	0.83	3.18
600°C 2h and 550°C 15 min	0.74	3.85	0.76	2.16
350°C 2h	0.71	3.71	0.74	1.94
400°C 2h	0.74	4.44	0.82	2.69
550°C 2h	0.69	3.79	0.75	1.96

The photoluminescence spectra of all sample are shown in Figure 5.12 found that PL intensity of 350°C 2h and 300°C 15 min shows the highest rate recombination of electron and hole. We describe here a comparison of the intensity becomes lower than single-layered TiO$_2$ electode that mean the recombination rate decreased.
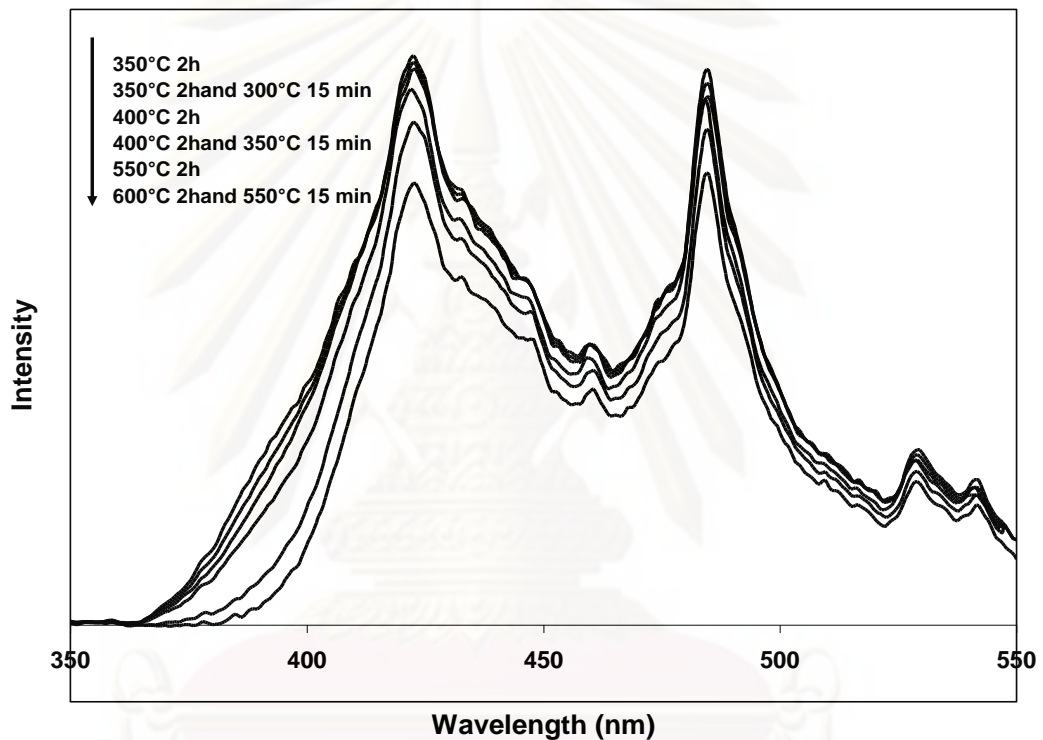
Figure 5.12 Photoluminescence spectra of TiO$_2$ sintered at various temperatures

5.2.2 Effect of thickness of TiO$_2$ film

We varied the thickness of TiO$_2$ electrode layer by varying number of coats of TiO$_2$ on the substrate. The numbers of coats of TiO$_2$ for this study were 200, 300, 400 and 500 coats. After coating, the electrode was sintered at 400 $^{\circ}$C 2h and 350°C 15 min.

Table 5.8 also shows the photovoltaic parameters of DSSC with different film thicknesses. From these results, the Isc of DSSC increase with the increase of theTiO_2 thin film thickness from 3.68 µm to11.19 µm.

The TiO_2 electrode sintered at $400^{\circ}C$ 2h and $350^{\circ}C$ 15 min, the thickness was about 11.19 µm gave the highest efficiency of 3.39%.

Table 5.8 Photovoltaic parameters of DSSC with TiO_2 electrode sintered at $400^{\circ}C$ 2h and $350^{\circ}C$ 15 min

Film Thickness (µm)	V_{OC} (Volt)	I_{SC} (mA/cm^2)	Fill Factor	Efficiency (%)
3.68	0.77	3.84	0.74	2.18
5.57	0.79	4.22	0.77	2.56
7.31	0.81	4.59	0.85	3.16
11.19	0.76	4.97	0.90	3.39

Figure 5.13 shown the cell efficiency increases linearly with the thickness increases. The efficiency of cell at various sintering temperature and various film thickness (see Figure 5.14) described that increasing of film thickness, increasing of the efficiency of TiO_2 electrode for every sintering temperature. Figure 5.15 showed the transmittances of the double-layered TiO_2 films. Transmitted light passing through the film increases with increasing wavelength. Compared with single-layered TiO_2 film and double-layered TiO_2 film resulted transmittance of the film decreased by the addition of the overlayer.

Figure 5.13 Efficiency of DSSC as a function of film thickness
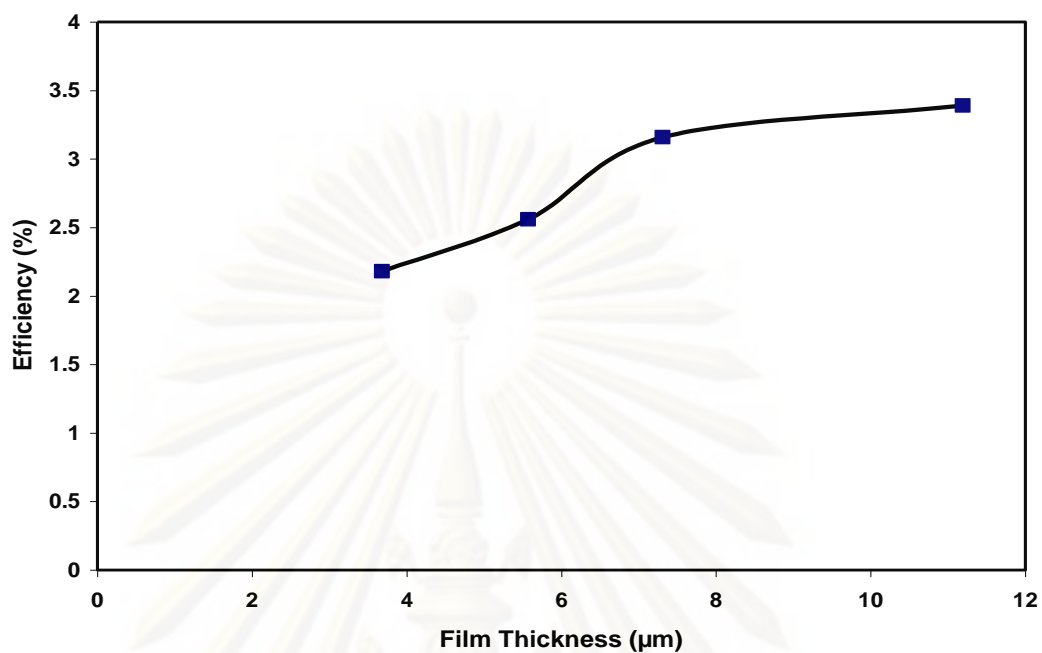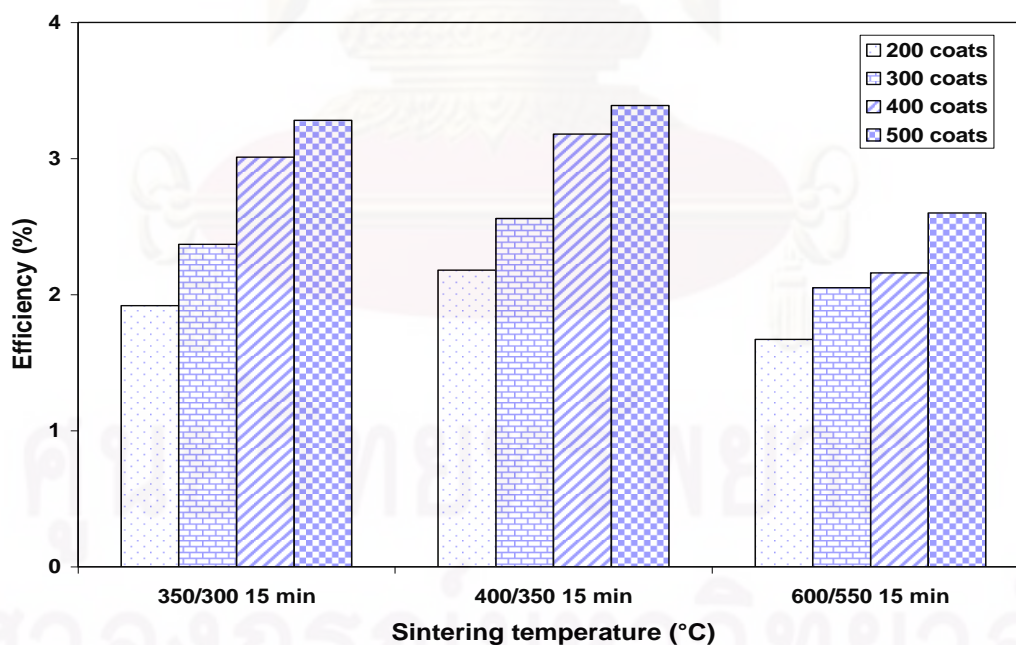

Figure 5.14 Efficiency of DSSC as a film thickness and sintering temperature of double-layered TiO_2 electrode
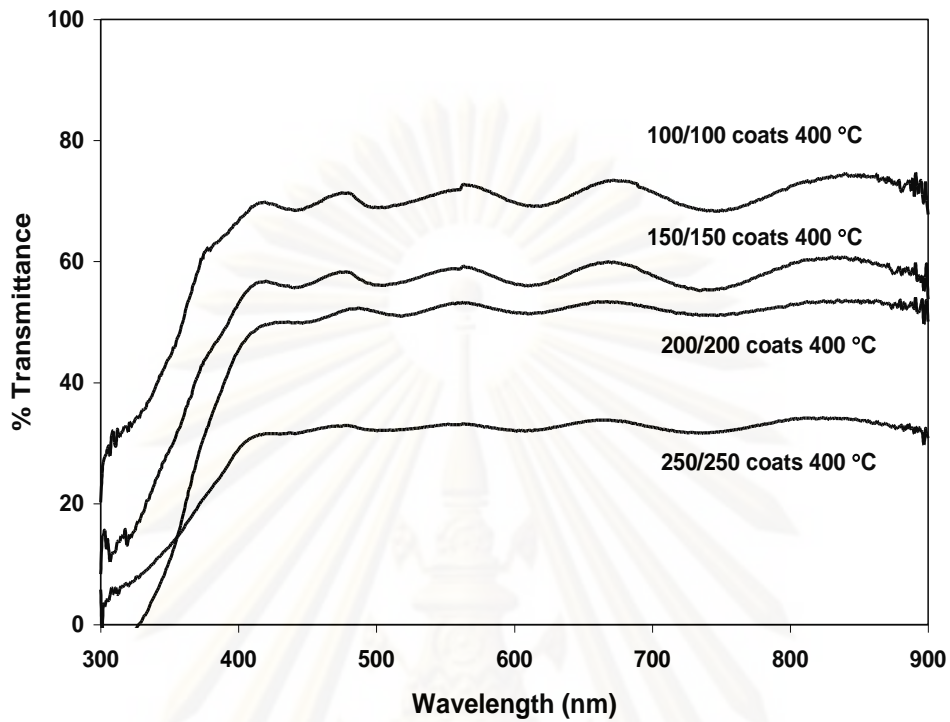
Figure 5.15 transmittance spectra of TiO$_2$ films with film thicknesses of 200 coats, 300 coats, 400 coats and 500 coats for double-layered

CHAPTER VI
CONCLUSIONS AND RECOMMENDATIONS
FOR FUTURE RESEARCH

In this chapter, section 6.1 provided the conclusion that obtained from the experimental results of the effect of sintering temperature, effect of thickness of TiO_2 electrode layer for single-layer and double-layer TiO_2 films on the performance of dye-sensitized solar cell. Additionally, recommendations for future study are presented in section 6.2.

6.1 Conclusion

6.1.1 Single-layered TiO_2 electrode

We have observed that the photovoltaic parameters of DSSC depend on sintering temperature and film thickness. We observed a maximum of short-circuit current density with a DSSC with a TiO_2 electrode calcined at $400^{\circ}C$ for two hours. The highest cell efficiency of 3.06% was observed in a DSSC with the thickest TiO_2 electrode layer (ca. 11 μm). The cell efficiency increased as the TiO_2 film thickness increased.

6.1.2 Double-layered TiO_2 electrode

We have observed that the photovoltaic parameters of DSSC depend on sintering temperature and film thickness. We investigated the improvement of photovoltaic performance by using double-layered TiO_2 film. With the addition of the overlayer to the double-layered TiO_2 film, the short-circuit current density of the DSSC were increased. Remarkably high cell efficiency of 3.39% was observed in a DSSC with the thickest TiO_2 electrode layer (ca. 11 μm).

6.2 Recommendations for future studies

From the previous conclusions, the following recommendations for future studies are proposed.

1. Improving efficiency of dye-sensitized solar cell by optimizing fabrication procedure.
2. Improving of the light harvest efficiency of dye-adsorbed TiO_2 electrodes by multi-layer (using a TiO_2 layer higher surface area increases the dye adsorption)

REFERENCES

Amornpitoksuk, P., and Leesakul, N. Dye Sensitized Solar Cell. <u>Songklanakarin J. Sci.</u>
<u>Technol</u> 25(4) (2003): 535-551.

Chang, H., Su, H. T., Chen, W. A., Huang, K. D., Chien, S. H., Chen, S. L., and Chen, C.
C. Fabrication of multilayer TiO_2 thin films for dye-sensitized solar cells with high
conversion efficiency by electrophoresis deposition. <u>Solar Energy</u> 84 (2010):
130–136.

Hore, S., Vetter, C., Kern, R., Smit, H., and Hinsch, A. Influence of scattering layers on
efficiency of dye-sensitized solar cells. <u>Solar Energy Materials & Solar Cells</u> 90
(2006):1176–1188.

Hossain, M. F., Biswas, S., and Takahashi, T. The effect of sputter-deposited TiO_2
passivating layer on the performance of dye-sensitized solar cells based on sol-
gel derived photoelectrode. <u>Thin solid films</u> 517 (2008): 1294-1300.

Huang, C. Y., Hsua, Y. C., Chena, J. G., Suryanarayanana, V., Leeb, K. M., and Ho, K.
C. The effects of hydrothermal temperature and thickness of TiO2 film on the
performance of a dye-sensitized solar cell. <u>Solar Energy Material & Solar Cells</u>
90 (2006): 2391-2397.

Kao, M. C., Chen, H. Z., Young, S. L., Kung, C. Y., and Lin, C. C. The effects of the
thickness of TiO_2 films on the performance of dye-sensitized solar cells. <u>Thin</u>
<u>Solid Films</u> 517 (2009): 5096–5099.

Karthikeyan, C. S., Thelakkat, M., and Willert-Porada, M. Different mesoporous titania
film for solid-state dye sensitized solar cells. <u>Thin Solid Film</u> 511-512 (2006):
187-194.

Koo, H. J., Beomjin, J. P., Yoo, K., Kim, K., and Park, N. G. Size-dependent scattering
efficiency in dye-sensitized solar cell. <u>Inorganica Chimica Acta</u> 361 (2008): 677-
683.

Lee, J. K., Jeong, B. H., Jang, S. I., Yeo, Y. S., Park, S. H., Kim, J. U., Kim, Y. G., Jang, Y. W., and Kim, M. R. Multi-layered TiO_2 nanostructured films for dye-sensitized solar cells. J Mater Sci: Mater Electron (2008).

Lee, J. K., Jeong, B. H., Jang, S. I., Kim, Y. G., Jang, Y. W., Lee, S. B., and Kim, M. R. Preparations of TiO_2 pastes and its application to light-scattering layer for dye-sensitized solar cells. Journal of Industrial and Engineering Chemistry 15 (2009): 724–729.

Lee, K. M., Suryanarayanana, V., and Ho, K. C. The influence of surface morphology of TiO_2 coating on the performance of dye-sensitized solar cells. Solar Energy Materials & Solar Cells 90 (2006): 2398–2404.

Lee, W. J., Ramasamy, E., and Lee, D. Y. Effect of electrode geometry on the photovoltaic performance of dye-sensitized solar cells. Solar Energy Material & Solar Cells (2008).

Lenzmann, F., and Kroon, J. Review: Recent Advances in Dye-Sensitized Solar Cells. Advances in OptoElectronics 10 (2007): 1755-1785.

Li, P., Wu, J., Lin, J., Huang, M., Huang, Y., and Li, Q. High-performance and low platinum loading Pt/Carbon black counter electrode for dye-sensitized solar cells. Solar Energy 83 (2009): 845-849.

Liqianga, J., Yichuna, Q., Baiqia, W., Shudana, L., Baojianga, J., Libina, Y., Weia, F., Hongganga, F., Jiazhong, S. Review of photoluminescence performance of nano-sized semiconductor materials and its relationships with photocatalytic activity. Solar Energy Materials & Solar Cells 90 (2006): 1773-1787.

Ngamsinlapasathian, S., Sreethawong, T., Suzuki, Y., and Yoshikawa, S. Single- and double-layered mesoporous TiO_2/P25 TiO_2 electrode for dye-sensitized solar cell. Solar Energy Material & Solar Cells 86 (2005): 269-282.

N-Park, G., Lagemaat, J., and Frank, A. Comparison of Dye-Sensitized Rutile- and Anatase-Based TiO_2 Solar Cells. The Journal of Physical chemistry B 104 (2000): 8989-8994.

O'Regan, B., and Grätzel, M. Low-cost high-efficiency solar cell based on dye-sensitized colloidal TiO_2 film. Nature 353 (1991): 737-740.

Patrocinio, A. O. T., Paterno, L. G., and Iha, N. Y. M. Layer-by-layer TiO_2 films as efficient blocking layers in dye-sensitized solar cells. Journal of Photochemistry and Photobiology A: Chemistry 205 (2009): 23-27.

Phani, G., Tulloch, G., Vittorio, D., and Skryabin, I. Titania solar cells: new photovoltaic technology. Renewable Energy Pergamon. (2001).

Shi, J., Liang, J., Peng, S., Xu, W., Pei, J., and Chen, J. Synthesis, Characterization and electrochemical properties of a compact titanium dioxide layer. Solid State Sciences 11 (2009): 433-438.

Su, C., Hong, B., and Tseng, C. Sol-gel preparation and photocatalysis of titanium dioxide. Catalysis Today 96 (2004): 119-126.

Xu, H., Tao, X., Wang, D. T., Zheng, Y. Z., and Chen., J. F. Enhanced efficiency in dye-sensitized solar cells based on TiO_2 nanocrystal/nanotube double-layered films. Electrochimica Acta 55 (2010): 2280–2285.

Yu, H., Zhang, S., Zhao, H., Will, G., and Liu, P. An efficient and low-cost TiO_2ncompact layer for performance improvement of dye-sensitized solar cells. Electrochimica Acta 54 (2009): 1319-1324.

APPENDICES

APPENDIX A

CALCULATION OF THE CRYSTALLITE SIZE

Calculation of the crystallite size by Debye-Scherrer equation

The crystallite size can be calculated from the width at half-height of the diffraction peak of XRD pattern using the Debye-Scherrer equation.

From Scherrer equation:

$$D = \frac{K\lambda}{\beta \cos\theta} \tag{A.1}$$

Where   D = Crystallite size, $\overset{\circ}{A}$

K = Crystallite-shape factor

λ = X-ray wavelength, 1.5418 $\overset{\circ}{A}$ for CuKα

θ = Observed peak angle, degree

β = X-ray diffraction broadening, radian

The X-ray diffraction broadening (β) is the pure width of a powder diffraction, free of all broadening due to the experimental equipment. Standard α-alumina is used to observe the instrumental broadening since its crystallite size is larger than 2000 $\overset{\circ}{A}$. The X-ray diffraction broadening (β) can be obtained by using Warren's formula.

From Warren's formula:

$$\beta^2 = B_M^2 - B_S^2 \tag{A.2}$$

$$\beta = \sqrt{B_M^2 - B_S^2}$$

Where B_M = Measured peak width in radians at half peak height.

B_S = Corresponding width of a standard material.

Example: calculation of the crystallite size of titania

The half-height width of (101) diffraction peak $\qquad$ = 1.48190°

$\qquad\qquad\qquad\qquad\qquad\qquad\qquad\qquad\qquad\qquad$ = 0.02586 radian

The corresponding half-height width of peak of titania = 0.003836 radian

The pure width = $\sqrt{B_M^2 - B_S^2}$

$\qquad\qquad\qquad$ = $\sqrt{0.02586^2 - 0.003836^2}$

$\qquad\qquad\qquad$ = 0.02557 radian

β $\qquad$ = 0.02557 radian

2θ $\qquad$ = 25.32°

θ $\qquad$ = 12.66°

λ $\qquad$ = 1.5418 A$^{\circ}$

The crystallite size $\qquad$ = $\dfrac{0.9 \times 1.5418}{0.02557 \cos 12.66}$ = 55.62 A$^{\circ}$

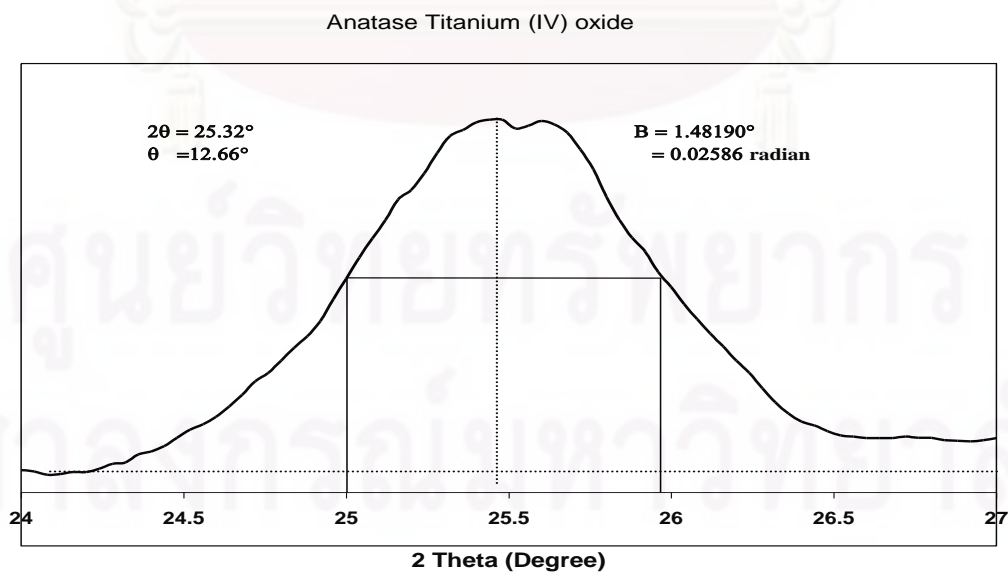$\qquad\qquad\qquad\qquad\qquad$ = 5.6 nm

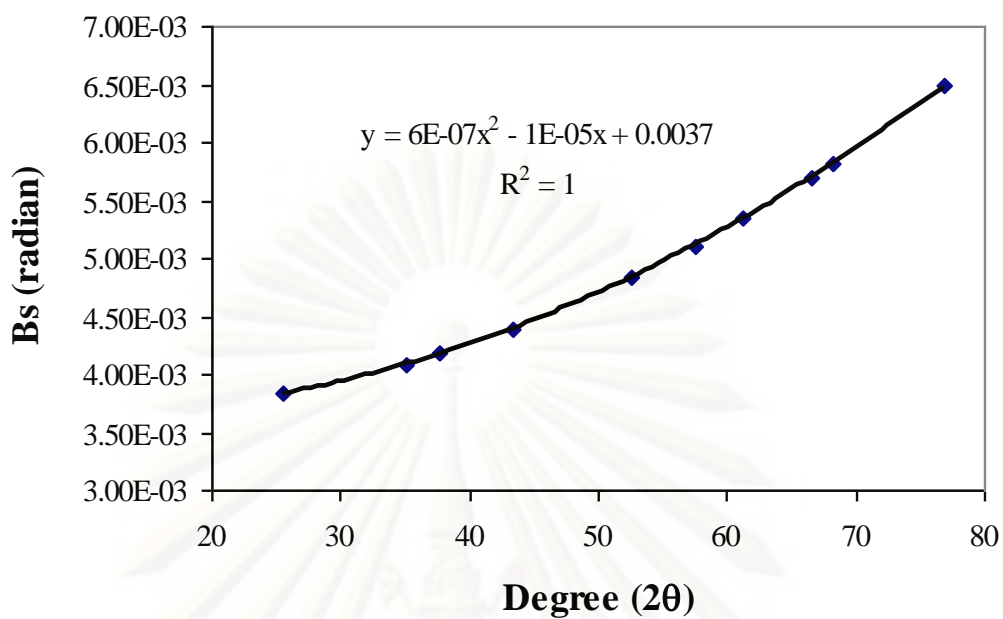Figure A.1 The (101) diffraction peak of titania for calculation of the crystallite size

Figure A.2 The plot indicating the value of line broadening due to the equipment. The data were obtained by using α-alumina as standard

APPENDIX B

CALCULATION OF WEIGHT FRACTION OF ANATASE, RUTILE AND
BROOKITE PHASE

The phase content of a sample was determined by XRD which can be calculated from the integrated intensities at 2θ values of 25.32°, 27.44° and 30.88° corresponded to the anatase, rutile and brookite phase, respectively.

The weight fraction of the phase content can be calculated by (Zhang and Banfield, 2000) as follows:

$$W_A = \frac{k_A A_A}{k_A A_A + A_R + k_B A_B}$$

$$W_R = \frac{A_R}{k_A A_A + A_R + k_B A_B}$$

$$W_B = \frac{k_B A_B}{k_A A_A + A_R + k_B A_B}$$

Where

W_A = weight fraction of anatase

W_R = weight fraction of rutile

W_B = weight fraction of brookite

A_A = the intensity of the anatase peak

A_R = the intensity of the rutile peak

A_B = the intensity of the brookite peak

K_A = the coefficients factor of anatase was 0.886

K_B = the coefficients factor of brookite was 2.721

Example: calculation of the phase content of TiO_2 sintered $300^{\circ}C$

Where

The integrated intensities of anatase (A_A)   = 775

The integrated intensities of rutile (A_R)   = 233

The integrated intensities of brookite (A_B)   = 65

The weight fraction of the phase content can be calculated by (Zhang and Banfield, 2000) as follows:

$$W_A = \frac{0.886(775)}{0.886(775) + (233) + 2.721(65)} = 0.62$$

$$W_R = \frac{233}{0.886(775) + (233) + 2.721(65)} = 0.22$$

$$W_B = \frac{2.721(65)}{0.886(775) + (233) + 2.721(65)} = 0.16$$

APPENDIX C

THE ELECTROCHEMICAL PROPERTIES OF DYE-SENSITIZED SOLAR
CELL

The electrochemical properties of dye-sensitized solar cell with various film
thickness and sintering temperature of TiO_2 electrode by I-V tester.

Table C.1 The electrochemical properties of TiO_2 electrode calcined at $300^\circ C$ with
various number of coats

Number of coats	V_{OC} (Volt)	I_{SC} (mA/cm^2)	Fill Factor	Efficiency (%)
200	0.68	2.71	0.65	1.23, 1.15
300	0.71	3.02	0.67	1.56, 1.32
400	0.71	3.43	0.69	1.80, 1.56
500	0.72	3.61	0.74	1.96, 1.88

Table C.2 The electrochemical properties of TiO_2 electrode calcined at $350^\circ C$ with
various number of coats

Number of coats	V_{OC} (Volt)	I_{SC} (mA/cm^2)	Fill Factor	Efficiency (%)
200	0.68	2.68	0.67	1.33, 1.11
300	0.70	3.34	0.70	1.66, 1.62
400	0.71	3.71	0.74	2.02, 1.86
500	0.69	4.29	0.79	2.55, 2.13

Table C.3 The electrochemical properties of TiO_2 electrode calcined at $400\,^\circ$C with various number of coats

Number of coats	V_{OC} (Volt)	I_{SC} (mA/cm^2)	Fill Factor	Efficiency (%)
200	0.73	3.51	0.71	1.97, 1.67
300	0.76	4.02	0.75	2.36, 2.22
400	0.74	4.44	0.82	2.74, 2.64
500	0.72	4.83	0.88	3.09, 3.03

Table C.4 The electrochemical properties of TiO_2 electrode calcined at $500\,^\circ$C with various number of coats

Number of coats	V_{OC} (Volt)	I_{SC} (mA/cm^2)	Fill Factor	Efficiency (%)
200	0.71	2.72	0.69	1.43, 1.23
300	0.72	3.41	0.73	1.83, 1.75
400	0.71	3.92	0.77	2.19, 2.09
500	0.71	4.46	0.82	2.66, 2.54

Table C.5 The electrochemical properties of TiO_2 electrode calcined at $550^{\circ}C$ with various number of coats

Number of coats	V_{OC} (Volt)	I_{SC} (mA/cm^2)	Fill Factor	Efficiency (%)
200	0.71	2.72	0.68	1.35, 1.27
300	0.72	3.31	0.71	1.72, 1.66
400	0.69	3.79	0.75	2.05, 1.87
500	0.71	4.22	0.79	2.40, 2.34

Table C.6 The electrochemical properties of TiO_2 electrode calcined at $600^{\circ}C$ with various number of coats

Number of coats	V_{OC} (Volt)	I_{SC} (mA/cm^2)	Fill Factor	Efficiency (%)
200	0.71	2.72	0.68	1.32, 1.30
300	0.72	3.22	0.70	1.67, 1.57
400	0.68	3.58	0.73	1.87, 1.73
500	0.71	3.91	0.78	2.19, 2.13

Table C.7 The electrochemical properties of TiO_2 electrode calcined at 350 2h and 300°C 15 min with various number of coats

Number of coats	V_{oc} (Volt)	I_{sc} (mA/cm^2)	Fill Factor	Efficiency (%)
200	0.78	3.33	0.74	1.93, 1.91
300	0.77	4.01	0.77	2.39, 2.35
400	0.79	4.74	0.82	3.09, 3.05
500	0.76	4.97	0.87	3.29, 3.27

Table C.8 The electrochemical properties of TiO_2 electrode calcined at 400 2h and 350°C 15 min with various number of coats

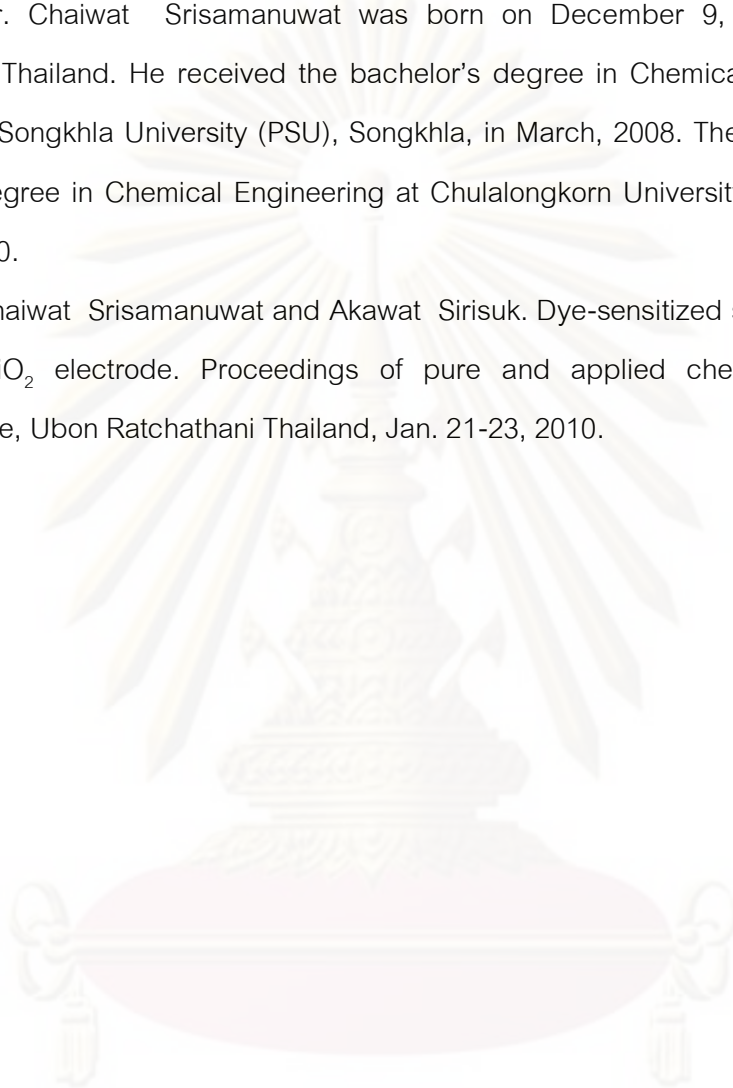| Number of coats	V_{oc} (Volt)	I_{sc} (mA/cm^2)	Fill Factor	Efficiency (%)
200	0.77	3.84	0.74	2.22, 2.14
300	0.79	4.22	0.77	2.69, 2.43
400	0.81	4.59	0.85	3.24, 3.08
500	0.76	4.97	0.90	3.51, 3.27

Table C.9 The electrochemical properties of TiO$_2$ electrode calcined at 600 2h and

550°C 15 min with various number of coats

Number of coats	V$_{oc}$ (Volt)	I$_{sc}$ (mA/cm^2)	Fill Factor	Efficiency (%)
200	0.76	3.01	0.73	1.79, 1.55
300	0.78	3.55	0.74	2.15, 1.95
400	0.74	3.85	0.76	2.24, 2.08
500	0.75	4.23	0.82	2.67, 2.53

VITA

Mr. Chaiwat Srisamanuwat was born on December 9, 1985 in Songkhla province, Thailand. He received the bachelor's degree in Chemical Engineering from Prince of Songkhla University (PSU), Songkhla, in March, 2008. Then he continued his master degree in Chemical Engineering at Chulalongkorn University and graduated in June, 2010.

Chaiwat Srisamanuwat and Akawat Sirisuk. Dye-sensitized solar cell with spray coated TiO_2 electrode. Proceedings of pure and applied chemistry international conference, Ubon Ratchathani Thailand, Jan. 21-23, 2010.